JOURNAL OF MATERIALS SCIENCE 27 (1992) 6249–6273

Review
Self-propagating high-temperature synthesis

J. SUBRAHMANYAM, M. VIJAYAKUMAR
Combustion Synthesis Group, Defence Metallurgical Research Laboratory, Hyderabad 500 258, India

Self-propagating high-temperature synthesis (SHS) and processes based on SHS are currently being developed the world over for the production of powders and near-net shape components of advanced materials. The research activities that have been and are being carried out in this field are reviewed here. Theoretical principles underlying SHS process, such as equlibrium computation and kinetics involving heat and mass transfer are described. General concepts about the SHS reaction mechanisms with a few illustrative examples are presented. Along with a detailed description of the processing techniques such as powder production, *in situ* consolidation and casting, a few of the novel techniques based on SHS are also elaborated.

Nomenclature

C_p	Combined heat capacity of the products
D	Diffusion coefficient, $D = D_o\, e^{-(E/RT)}$
E	Activation energy
f	Fraction melted
$\Delta H^r_{T_o}$, Q	Enthalpy of the reaction at temperature, T_o
k	Reaction rate constant, $k = k_o\, e^{-(E/RT)}$
n	Order of the reaction
p_B	Partial pressure of the reactant gas B
R	Universal gas constant
S	Surface area of the solid reactant
T_{ad}	Adiabatic temperature
T_o	Initial temperature
T_m	Melting point
T_b	Boiling point
v	Velocity of wave propagation
α	Thermal diffusivity
α_c	Parameter delineating combustion regimes
η	Fraction converted

1. Introduction

Self propagating high-temperature synthesis (SHS) is the term presently being used to describe a process in which initial reagents, when ignited, spontaneously transform into products, due to the exothermic heat of reaction. Several other terminologies like combustion synthesis, gasless combustion, self propagating combustion, self propagating exothermic reactions are used for describing the same process. This process, an offshoot of pyrotechnics, evolved from the studies conducted on the combustion of solid cylindrical compacts such as Ti–B mixtures by Merzhanov *et al.* [1–6] at the Institute Chemical Physics of USSR Academy of Sciences. Activities in America and other places were started after the publication by Crider [7] about this technique. He gave a detailed account of the salient features of the process and the different groups involved in SHS research in the Soviet Union. Frankhouser *et al.* [8] published a monograph on gasless combustion synthesis giving a fairly detailed account of the Soviet research activities in the field. Sheppard [9] gave a popular account of Soviet work and the current activities in American research establishments. McCauley [10] recently presented a historical and technical perspective.

Detailed technical reviews appeared recently in the literature by Holt [11], Munir [12], Munir and Anselmi Tamburini [13], Merzhanov [14] and Yi and Moore [15]. It is a formidable task to attempt a comprehensive review of all the literature available on SHS and this is not aimed at here. Instead, an effort is made to review the essential principles guiding the SHS research in a coherent fashion, along with a few relevant examples from the literature.

1.1. Generalized SHS reactions

Two general SHS processes have been recognized: (1) processes in which layerwise combustion occurs, and (2) processes wherein volumetric combustion occurs [16]. Conventional combustion processes are generally volumetric, wherein reactions occur in a volume generating heat and required products. SHS reactions occur in general by propagation of a combustion wave (layerwise) with a definite velocity through a reactant pellet converting it into products. A generalized SHS reaction can be written as [16]

$$\underbrace{\sum_{i=1}^{m} a_i X_i}_{\text{Element (Fuel)}} + \underbrace{\sum_{j=1}^{n} b_j Y_j}_{\text{Element (Oxidizer)}} \rightarrow \underbrace{Z}_{\text{Product}} \qquad (1)$$

where X = Ti, Zr, Hf, V, Nb, Ta, Mo, W, etc. Y = B

(Z = borides), C (Z = carbides), N (Z = nitrides), Si (Z = silicides), S (Z = sulphides), etc.
Mixed compounds are obtained when m and n are greater than one. For e.g. $Nb_xZr_{1-x}N$, $Nb_xZr_{1-x}C_yN_z$, etc. Fuel and oxidizer are indicated to show the similarity of this type of reaction with the conventional combustion processes.

By a combination of metallothermic reactions with Equation 1, two types of reaction can be visualized

$$\underset{\text{Compound for reduction}}{MeX_m} + \underset{\text{Reducing agent}}{Y} \rightarrow \underset{\text{Required product}}{MeY_n} + \underset{\text{By-product}}{YX_k} \quad (2)$$

e.g. $$WO_3 + 3B \rightarrow WB + B_2O_3$$

$$\underset{\substack{\text{Compound for reduction}}}{MeX_m} + \underset{\text{Reducing agent}}{Me'} + \underset{\text{oxidizer}}{X'} \rightarrow \underset{\text{Required product}}{MeX'_n} + \underset{\text{By-product}}{Me'X} \quad (3)$$

e.g. $$MoO_3 + 2Al + 2Si \rightarrow MoSi_2 + Al_2O_3$$

In these processes one of the elements is obtained by metallothermic reduction. One such reaction is the well-known thermite reaction

$$Fe_2O_3 + 2Al \rightarrow 2Fe + Al_2O_3 \quad (4)$$

which generates temperatures above the melting point of Al_2O_3.

1.2. Merzhanov's classifications of SHS physicochemical mechanisms

An important parameter in the SHS reactions is the adiabatic temperature, T_{ad}. This is the temperature to which the products are raised under adiabatic conditions as a consequence of the evolution of heat due to the chemical reaction.

Merzhanov [17] made a physico-chemical classification of SHS mechanisms for a binary system based on the adiabatic temperatures and melting and boiling points of the reactants. This is shown in Table I. If the adiabatic temperature is less than the boiling point of both the elements participating in the reaction, no vapour phase is present in the reaction. However, an ideal gas-free combustion can be realized only when the ratio of the vapour pressure at the adiabatic temperature to the atmospheric pressure tends to zero. Two examples are shown in Table I. For the combustion of TiB_2, even though the adiabatic temperature is less than the boiling point of both the elements, the vapour pressure of the elements at the adiabatic temperature is high, and hence high pressures are needed to make it a gasless combustion. In the case of MoB, however, the vapour pressure at the adiabatic temperatures is so low that it is an ideal gasless combustion even in vacuum.

When the adiabatic temperature is greater than the melting point of the reactants but lower than the boiling point, reactions occur in liquid phase. If the adiabatic temperature lies in between the melting point of the components, the molten component spreads at a high rate in the compact, resulting in the highest velocity of combustion. Complete solid state combustion occurs when the melting points are less than the adiabatic temperature leading to lowest combustion velocities. One of the widely used combustion

TABLE I Physicochemical classification of SHS reaction mechanisms for a two component system [17]

Relation between T_{ad}, T_m and T_b	Characteristics of the system	Examples
1. $T_{ad} < T_b^i$ $i = 1, 2$	Ideal gas free combustion occurs if $[P(T_{ad})/P_o] \rightarrow 0$	1. $Ti + 2B = TiB_2$ $T_{ad} = 3200$ K ($T_o = 293$ K) $P_{Ti}(3200\text{ K}) = 8$ kPa $P_B(3200\text{ K}) = 0.4$ kPa Gasless reaction only at high pressures 2. $Mo + B = MoB$ $T_{ad} = 1750$ K ($T_o = 293$ K) $P_{Mo}(1750\text{ K}) = 10^{-7}$ Pa $P_B(1750\text{ K}) = 10^{-6}$ Pa Gasless reaction even in high vacuum
2. $T_m^i < T_{ad} < T_b^i$ $i = 1, 2$	Both components in liquid state	$Ni + Al = NiAl$ $T_{ad} = 1910$ K Ni: T_m(K) 1726, T_b(K) 3373 Al: T_m(K) 933, T_b(K) 2773
3. $T_m^1 < T_{ad} < T_m^2$	Solid + liquid reaction. Highest propagation velocity	$Ti + C = TiC$ $T_{ad} = 3210$ K $T_m^{Ti} = 1933$ K $T_m^C = 3973$ K
4. $T_{ad} < T_m^i (i = 1, 2)$	Both components in solid state. Lowest combustion velocity. Difficult combustion	$2Ta + C = Ta_2C$ $T_{ad} = 2600$ K $T_m^{Ta} = 3269$ K $Ta + C = TaC$ $T_{ad} = 2700$ K
5. $T_b^1 < T_{ad} < T_b^2$	One component in the gaseous phase and the other in condensed state. Widely used process	Formation of nitrides, hydrides, sulphides, selenides, phosphides etc.
6. $T_{ad} > T_b^i$ $i = 1, 2$	Both reactants in gas phase and solid product	Very few systems studied. Mg + S

processes is the reaction between a condensed phase and gas phase. This happens when one of the components is in the gas phase. Finally, gas-phase reactions can yield solid products but such system are not studied extensively.

This classification is limited only to two-component systems and the physical state of the product is neglected in the mechanisms. Nevertheless the knowledge of the adiabatic temperature and the physico-chemical state of the reactants gives sufficient basis for visualizing possible reaction mechanisms. Table II presents these data for a number of carbides, borides, silicides and nitrides. Melting points of the products and approximate values of the combustion velocities are also included here.

1.3. Terminology

As already seen, gasless combustion is a specific process under the general description of SHS. Because the number of processes and techniques based on SHS are growing rapidly, it is probably time to define certain precise terms, depending on the physico-chemical process or the technique by which the products are obtained. From Table I each physico-chemical condition of the reactants can be defined as a distinct process. Certain established terms already in use in SHS literature are also included for completeness.

1. Gasless combustion: combustion when the condition $T_{ad} < T_b^i$ is satisfied. This includes combustion processes which can be made gasless by the application of external pressures greater than $P(T_{ad})$.
2. Liquid phase combustion: the condition $T_m^i < T_{ad} < T_b^i$ is to be satisfied.
3. Solid–liquid combustion: one of the components is the liquid phase.
4. Solid–solid combustion: all the components are in the solid state.
5. Solid–gas combustion: at least one component is in the gas phase.
6. Combustion condensation: all reactants are in the vapour phase with the product in the solid state.
7. Combustion casting: products reach sufficiently high temperature so that they can be poured into a casting.
8. Combustion coating: coatings obtained involving SHS reactions.
9. Combustion consolidation: consolidation of SHS products utilizing the exothermic heat available in the reactions.
10. Combustion roasting: oxidation of sulphide ores with the exothermic heat.
11. Combustion milling: milling of exothermic reactants to obtain products. The reaction is initiated by continuous impact during milling.
12. Thermal explosion: a volumetric reaction that occurs when a reactant compact is heated rapidly in a furance. This is in contrast to the layerwise reaction in the usual SHS reactions.
13. Chemical furnace: SHS reactants can be used as a furnance because the reaction generates high tempertures. This is often used to initiate reactions with low T_{ad}.
14. Thermal and chemical wave: conceptual terms describing the propagation of heat and the extent of chemical conversion in a combustion wave. The two are interdependent.
15. After burn: secondary luminescence generated after the passage of a combustion wave due to lag between the thermal and chemical waves.
16. Homogeneous combustion: combustion in which thermal and chemical waves coincide with an associated narrow combustion zone.
17. Heterogeneous combustion: combustion in which thermal and chemical waves do not coincide with associated wide reaction zones.

Such appropriate terminology can also be defined to represent specific combustion processes. The terms combustion synthesis and SHS can be used to represent the general or overall process.

1.4. Advantages

There are several advantages offered by the SHS process. The basic advantage is, of course, the self generation of the energy required for the process. This is in marked contrast with the highly energy-intensive processes used for obtaining the same refractory compounds – long hours of reaction at high temperatures in furnaces or plasma reactors. In addition to the negligible energy requirement, simple and inexpensive equipment is sufficient for carrying out SHS reactions. As very high temperatures are reached in many reactions, all the volatile impurities evaporate at these temperatures producing high-purity products. The process can be used not only for producing refractory powders but also to make near net-shape components by utilizing the exothermic heat with processes such as casting, consolidation and coating.

The process offers high productivity as it has the highest reaction rates. The usual problems with scaling up of the process are not encountered in SHS; in fact, reactions approach complete conversion with larger quantities, resulting in better yields of products. The process has produced unique products – a new hitherto unknown cubic tantalum nitride with high hardness has been reported [18]. Several other process adaptations are possible and some of these are described later.

The process generates immense theoretical interest with reaction propagation rates in the formation of carbides and borides reaching $0.25\ m\ s^{-1}$, where the diffusivity values are of the order of $10^{-10}\ cm^2\ s^{-1}$. It provides challenging opportunities to solve the heat and mass transfer equations, to obtain conditions for self propagation and to simulate the conditions for the process for obtaining the desired products.

2. Theory

In general, SHS process is mass and energy transport limited. In these reactions, energy is self generated. The maximum temperature, T_{ad}, can be obtained from thermochemical calculations assuming an adiabatic system. The nature and amount of different species in

TABLE II Combustion data for binary element reactions [13, 21]

	B: m.p. 2573 K, b.p.	C: m.p. 3823 K, b.p. 5100 K	Si: m.p. 1683 K, b.p. 2623 K	N
Ti: m.p. 1933 K b.p. 3560 K	TiB (1) 2–18 cm s^{-1} (2) 3350 K (4) 3×10^{2} mm Hg (3) 2500(d) K (5) 27	TiC (1) 0.8–12 cm s^{-1} (2) 3210 K (4) 1.6×10^{2} mm Hg (3) 3210 K (5) 3.2×10^{-4} mm Hg	Ti_5Si_3 (1) 1.9 cm s^{-1} (2) 2500 K (4) 1.6 mm Hg (3) 2403 K (5) 3.6 mm Hg	TiN (2) 4900 K (4) 3.7×10^{4} mm Hg (5) 3223 K –
Ti	TiB_2 (1) 2–18 cm s^{-1} (2) 3190 K (4) 1.4×10^{2} mm Hg (3) 3190 K (5) 10 mm Hg		$TiSi$ (1) 1.44 cm s^{-1} (2) 2000 K (4) 9.1×10^{-3} mm Hg (3) 1843 K (5) 0.03 mm Hg	
Zr: m.p. 2125 K b.p. 4650 K	ZrB_2 (1) 1–8.1 cm s^{-1} (2) 3310 K (4) 1.6 mm Hg (3) 3473 K (5) 21 mm Hg	ZrC (1) 2.0 cm s^{-1} (2) 3400 K (4) 2.9 mm Hg (3) 3803 K (5) 2.2×10^{-2} mm Hg	Zr_5Si_3 (1) 2.0 cm s^{-1} (2) 2800 K (4) 0.036 mm Hg (3) 2483 K (5) 27 mm Hg	ZrN (1) 1–3 cm s^{-1} (2) 4900 K (4) 1.5×10^{3} mm Hg (3) 3253 K mm Hg
Hf: m.p. 2500 K b.p. 4875 K	HfB_2 (1) 0.2–2.5 cm s^{-1} (2) 3520 K (4) 7.4 mm Hg (3) 3523 K (5) 69 mm Hg	HfC (1) 0.7 cm s^{-1} (2) 3900 K (4) 53 mm Hg (3) 4163 K (5) 3.8×10^{-2} mm Hg	–	HfN (2) 5100 K (4) 3.7×10^{3} mm Hg (3) 3273 K – mm Hg
V: m.p. 2163 K b.p. 3653 K	VB_2 (2) 2670 K (4) 2.9 mm Hg (3) 2673 K (5) 0.18 mm Hg	VC (2) 2400 K (3) 0.24 mm Hg (3) 2921 K (5) 4.3×10^{-8} mm Hg	– –	VN (2) 3500 K (4) 4.74×10^{2} mm Hg –
Nb: m.p. 2741 K b.p. 5015 K	NbB_2 (1) 0.32–0.62 cm s^{-1} (2) 2400 K (4) 2×10^{-5} mm Hg (3) 3273 K (5) 0.01 mm Hg	NbC (3) 2800 K (4) 3×10^{-3} mm Hg (3) 3886 K (5) 7×10^{-6} mm Hg	$NbSi_2$ (2) 1900 K (4) 10^{-9} mm Hg (3) 2203 K (5) 10^{-2} mm Hg	Nb_2N (2) 2670 K (4) 7×10^{-4} mm Hg (3) 2323 K –
Nb	–	Nb_2C (2) 2600 K (4) 3×10^{-4} mm Hg (3) 3308 (5) 6.7×10^{-7} mm Hg	–	NbN (2) 3500 K (4) 1.4 mm Hg
Ta: m.p. 3269 K b.p. 5698 K	TaB_2 (1) 0.8 cm s^{-1} (2) 2700 K (4) 1.5×10^{-5} mm Hg (3) 3310 K (5) 0.24 mm Hg	TaC (2) 2700 K (4) 1.5×10^{-5} mm Hg (3) 4258 K (5) 2×10^{-6} mm Hg	$TaSi_2$ (2) 1800 K (4) 4×10^{-13} mm Hg (3) 2473 K (5) 2.5×10^{-3} mm Hg	TaN (1) 0.5–1.7 cm s^{-1} (2) 3360 K (4) 1.4×10^{-2} mm Hg (3) 3360 K –
Cr: m.p. 2130 K b.p. 2945 K	CrB_2 (2) 2470 K (4) 55.3 mm Hg (3) 2473 K (5) 0.02 mm Hg	– – –	$CrSi_2$ (2) 1800 K (4) 0.06 mm Hg (3) 1748 K (5) 2.5×10^{-3} mm Hg	– –
Mo: m.p. 2890 K b.p. 4885 K	MoB (1) 0.65 cm s^{-1} (2) 1800 K (4) 4×10^{-9} mm Hg (3) 2823 K (5) 10^{-6} mm Hg	Mo_2C (2) 1000 K (4) 2×10^{-24} mm Hg (3) 2795 K (5) 6×10^{-30} mm Hg	$MoSi_2$ (1) 0.4 cm s^{-1} (2) 1900 K (4) 4×10^{-8} mm Hg (3) 2293 K (5) 10^{-2} mm Hg	
W m.p. 3683 K b.p. 6203 K	WB (2) 1700 K (4) 3×10^{-16} mm Hg (3) 3070 K (5) 10^{-7} mm Hg	WC (2) 1000 K (4) 2×10^{-34} mm Hg (3) 3058 K (5) 6×10^{-30} mm Hg	WSi_2 (2) 1500 K (4) 10^{-19} mm Hg (3) 2433 K (5) 10^{-5} mmHg	– –

Notes: (1) Approximate combustion velocity for the formation of, for example, TiB.
(2) Adiabatic temperature, T_{ad}, for the formation of, for example, TiB
(3) Melting point of, for example, TiB.
(4) Vapour pressure of, for example, Ti at T_{ad}.
(5) Vapour pressure of, for example, B, at T_{ad}.

equilibrium at the adiabatic temperature can be computed by techniques such as global free-energy minimization. Further, the energy liberated by the chemical reaction is distributed to the surroundings by heat conduction, convection and radiation. In addition, mass transport controls the chemical reaction rates and is, in turn, controlled by the reaction mechanism. These three parameters namely energy generation, energy distribution and mass transport, interactively control an SHS process. These aspects are discussed in this section.

2.1. Thermochemical calculations

Thermodynamic evaluation of the combustion system can give quite useful information. The enthalpy of reaction, ΔH^{r}_{298} is an important parameter which decides whether or not a chemical reaction is self propagating. At low values of enthalpy change, no combustion can occur, and at very high values, combustion occurs with self propagation. This heat of reaction is utilized in raising the temperature of the products of combustion and the maximum temperature thus attained, the adiabatic temperature, T_{ad}, can be calculated from the heat balance condition [19–21]

$$\Delta H^{r}_{T_o} = \int_{T_o}^{T_{ad}} C_p \, dT \qquad (5)$$

where $\Delta H^{r}_{T_o}$ is the enthalpy of reaction at T_o and C_p is the combined heat capacity of the products. If the product constituents undergo any phase transformations below the T_{ad} thus calculated, then the corresponding changes in the enthalpy and heat capacities have to be taken into account and T_{ad} recalculated in a part-wise manner. For instance, if one of the products is in the molten condition, then its melting point itself is the T_{ad} and the fraction in molten condition, f, can be obtained from the equation,

$$\Delta H^{r}_{T_o} = \int_{T_o}^{T_m} C_p \, dT + f\Delta H_m \qquad (6)$$

where ΔH_m is the latent heat of fusion.

In these calculations, it is assumed that all the heat generated by the reaction goes only to raise the temperature of the products and there is no loss of heat to the surroundings, meaning it is a "closed system". It is also assumed that the difference between the heat capacity of the products and the reactants, due to the rise in temperature, is zero (Neumann–Kopp rule). In additon, it is assumed that the reaction goes to completion. Thus T_{ad} is only a measure of the exothermicity of the reaction and defines the upper limit for any combustion system.

From the knowledge of the T_{ad}, certain systems can either be eliminated for experimentation or combined with other more exothermic reactions to make them amenable for SHS. Merzhanov has suggested an empirical criterion that if $T_{ad} < 1500$ K, combustion does not occur, and if $T_{ad} > 2500$ K, self-propagating combustion occurs. In the range $1500\,K < T_{ad} < 2500\,K$, a combustion wave cannot propagate but can be made to do so by special techniques such as initial heating of the reactants.

In systems where high T_{ad} can be obtained, the products can be consolidated after the synthesis. Such a combined synthesis and consolidation, going from the initial reactants to a final dense product, is an ideal condition for SHS, because it optimally utilizes the available exothermic heat. In order to achieve a high degree of consolidation, it is advantageous to maintain one of the constituents in a partially molten condition. T_{ad} can be appropriately tailored for this purpose either by heating the initial reactants or by the addition of suitable diluents. Such a procedure can also be used to maintain the product in the completely molten state, allowing combustion casting.

The effect of initial temperature and the addition of diluents to the initial mixture on the adiabatic temperature for the preparation of TiB_2 composites is reported by Subrahmanyam *et al.* [19]. Fig. 1 shows the effect of addition of B_4C to the initial mixture, on the adiabatic temperature and amounts of molten fractions of TiB_2 and B_4C formed. It can be seen that about 0.5 mol B_4C addition reduces the T_{ad} from the melting point of TiB_2 (3193 K) to the melting point of B_4C (2743 K). This figure clearly shows the possibility of closely monitoring the adiabatic temperature and the amount of molten fraction by the addition of diluents. Similar calculations for TiC formation from the elements are reported by Holt and Munir [20]. The adiabatic temperature of several systems have been calculated [21]. Table III presents a comparison of T_{ad} with measured combustion temperatures [14].

2.2. Generalized equilibrium computation

The preceding thermochemical calculations are adequate only for simple chemical reactions. However, many real chemical reactions involve various species with definite stability at high temperatures and pressures. Consequently, a number of simultaneous reactions will be occurring, starting from the same initial reactants. In such situations, simultaneous equilibria

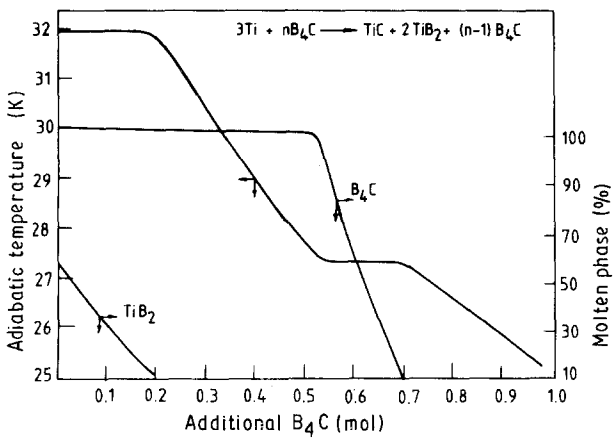

Figure 1 Effect of addition of excess moles of B_4C to reactant mixture on the adiabatic temperature and the amount of molten phases formed [19].

TABLE III Comparison of calculated and experimental combustion temperatures in SHS systems [14]

Reaction	T (calc.) (K)	T (expt.) (K)
Ni + Al + NiAl	1910	1910
Co + Al → CoAl	1900	1880
Ti + Si → TiSi	2000	1850
Ti + 2Si → $TiSi_2$	1800	1770
Nb + 2Si → $NbSi_2$	1900	1880
Mo + 2Si → $MoSi_2$	1900	1920
5Ti + 3Si → Ti_5Si_3	2500	2350
Nb + C → NbC	2800	2650
2Ta + C → Ta_2C	2600	2550

are to be solved along with the mass balance constraint to obtain equilibrium composition at any given temperature and pressure. Several computer-based techniques have been developed for this purpose which include the free-energy minimization and equilibrium constant methods [22]. The usefulness of such a calculation in SHS reactions is illustrated by the following two examples [23].

Table IV presents the results of equilibrium calculation on the $TiCl_4$ + Mg system to produce titanium metal. Amounts of various species in equilibrium at different temperatures and pressures are given; 20% Mg is the stoichiometric composition. Increasing the magnesium in the initial mixture above the stoichiometric value decreases T_{ad} and increases the yield of titanium. Increasing the total pressure increases both T_{ad} and the yield of titanium. The authors recommended stoichiometric mixtures and a total pressure greater than 40 atm as optimum conditions. This combination gives 95% yield and minimum unreacted magnesium in the product.

Table V presents the T_{ad} and the yield of AlN at three different total pressures for different nitrogen to aluminium (N/Al) ratios from three different nitrogen precursors in a Al–N–H system. It can be seen that the T_{ad} as well as AlN yield increases with increase in total pressure. The AlN yield increases and T_{ad} decreases with increase in N/Al ratios at any pressure. The low yield at low N/Al ratios was attributed to the easy dissociation of AlN formed at high T_{ad}. Higher pressures and low T_{ad} reduces the dissociation of AlN giving better yields.

2.3. Kinetics of combustion reactions

The exothermic chemical reactions generate heat and the combustion wave passes through the reactant pellet converting it into products. The heat is transferred to the material ahead of the wave front providing necessary heat for initiating the reaction. Some of it is also lost to the surroundings. The conversion rate of the reactants into products may or may not coincide with the rate of the heat wave propagation resulting in a variety of combustion modes. In general, developing a theory or process modelling for SHS is quite complicated in view of the heterogeneous systems and multidimensional unsteady state heat and mass transfer problem involving moving boundaries [24–32]. Considerable work has been done in Soviet Union to analytically solve the equations using simplifying assumptions [24, 32]. Thus, they have derived expressions, for example, for velocity of combustion, which can be of great help in understanding the mechanisms of combustion as well as in carrying out experimental work.

TABLE IV Equilibrium composition and yield of titanium for different initial compositions and pressures [23]

Composition (%)		$Ti^{initial}$ (g atom/ kg mixture)	p (atm)	T_{ad} (K)	Equilibrium products (g mol/kg mixture)						Yield of Ti (%)
Mg	$TiCl_4$				Hg(g)	MgCl	$MgCl_2$(g)	$MgCl_2$(s)	$TiCl_2$	Ti(s)	
20	80	4.216	1.0	1542	0.084	1.116	1.321	5.701	0.840	3.368	79.88
			2.0	1624	0.080	1.042	1.017	6.083	0.799	3.409	80.86
			5.0	1746	0.069	0.870	0.664	6.620	0.702	3.506	83.16
			10.0	1852	0.054	0.681	0.436	7.052	0.594	3.615	85.74
			20.0	1963	0.019	0.268	0.164	7.771	0.355	3.856	91.46
			30.0	2021	0.008	0.129	0.085	8.001	0.275	3.937	93.38
			40.0	2046	0.005	0.068	0.051	8.100	0.240	3.971	94.19
			50.0	2057		0.042	0.036	8.143	0.224	3.986	94.51
			60.0	2062		0.029	0.028	8.165	0.216	3.994	94.73
			70.0	2065		0.021	0.022	8.178	0.211	3.998	94.83
22	78	4.111	1.0	1530	0.222	1.737	1.246	5.840	0.265	3.844	93.50
			2.0	1608	0.225	1.659	0.950	6.211	0.229	3.881	94.40
			5.0	1718	0.232	1.493	0.608	6.713	0.154	3.957	96.25
			10.0	1800	0.246	1.322	0.390	7.085	0.085	4.026	97.93
			20.0	1868	0.288	1.102	0.222	7.401	0.031	4.080	99.24
			30.0	1897	0.328	1.021	0.153	7.544	0.014	4.097	99.66
			40.0	1912	0.361	0.941	0.116	7.628	0.008	4.103	99.80
			60.0	1930	0.411	0.832	0.077	7.725	0.005	4.108	99.93
24	76	4.006	1.0	1453	0.756	2.235	0.728	6.539	0.017	3.988	99.55
			2.0	1507	0.820	2.094	0.517	6.436	0.010	3.995	99.72
			5.0	1574	0.938	1.847	0.304	6.779	0.005	4.001	99.87
			10.0	1620	1.049	1.620	0.190	7.008		4.004	99.95

TABLE V Adiabatic temperature and equilibrium yeild of AlN in Al–N–H system for different N/Al ratios and initial pressures [23]

System	N/Al	P(atm)					
		1		10		100	
		T(K)	η_{AlN} (%)	T(K)	η_{AlN} (%)	T(K)	η_{AlN} (%)
Al + N_2	1.231	2700	67.8	3030	82.1	3620	90.3
	1.453	2650	70.0	3050	83.9	3600	91.2
	1.850	2630	72.3	2990	86.6	3470	94.0
	2.000	2620	74.2	2950	88.8	3380	95.7
	3.280	2560	80.5	2790	95.0	3000	99.3
	3.910	2330	83.9	2700	97.3	2790	100.0
	8.210	2180	100.0	2180	100.0	–	–
Al + NH_3	1.012	2360	89.0	2590	93.0	2700	98.0
	1.100	2350	91.4	2560	95.4	2700	99.0
	1.405	2250	97.9	2340	99.4	2360	100.0
	1.649	2060	99.8	2070	100.0	–	–
	1.937	1800	100.0	–	–	–	–
Al + N_2H_4	1.032	2480	74.1	2720	87.2	3040	93.2
	2.144	2400	87.4	2630	93.1	2700	99.7
	3.740	2270	96.8	2360	99.5	2390	100.0
	4.790	1990	100.0	2080	100.0	–	–

The equation for heat conductivity with a chemical source of heat can be written as

$$\frac{\partial T}{\partial t} = \alpha \nabla^2 T + \frac{Q}{C_p} \phi(T, \eta) \quad (7)$$

where α is the thermal diffusivity, Q is the enthalpy of the reaction, C_p is the combined heat capacity of the products and $\phi(T, \eta)$ is the rate of the reaction. Heat losses to the surroundings by convection and radiation are neglected in the above equation. Before proceeding to a discussion on the solutions to this equation, a brief description on the rates of the reaction, which determine the time and temperature dependence of the heat source term, follows.

2.3.1 Reaction rate

In Equation 7, generally

$$\phi(T, \eta) = \frac{d\eta}{dt} \quad (8)$$

is the reaction rate and η is the fraction converted. A general approach has been to use either Arrhenius kinetics or diffusion kinetics to describe the reaction rate. Khaikin [24] utilized empirical equations of the type

$$\phi(T, \eta) = k_o \theta(\eta) e^{-(E/RT)} \quad (9a)$$

where

$$\theta(\eta) = \eta^{-n} e^{-m\eta} \quad (9b)$$

to explain peculiarities of combustion. In Equation 9a and b, E is the activation energy and n is the order of the reaction. Values of m and n are defined depending on whether the reaction rate follows a linear ($m = n = 0$), parabolic ($m = 0, n = 1$) or logarithmic ($m \neq 0, n = 0$) law. These approaches can give useful results to correlate the experimental data, and explain the peculiarities of combustion wave modes. However, it is appropriate to choose the right kinetic equation depending on the reaction mechanism. Elaborate discussion on such rate equations is out of scope of this review, but a brief discussion is presented here along with simplified rate equations.

Depending on the physical state of reactants at the adiabatic temperature, SHS reactions can be classified in the following way.

solid–solid reactions

$$A(s) + B(s) = AB(s) \quad (10)$$

Solid–liquid

$$A(s) + B(l) = AB(s) \quad (11)$$

Liquid–liquid

$$A(l) + B(l) = AB(s, l) \quad (12)$$

Solid–gas (includes liquid + gas)

$$A(s, l) + B(g) = AB(s) \quad (13)$$

The molar volume change from the reactants to products plays an important role.

Solid–solid reactions are essentially diffusion controlled. Wagner [33] proposed a parabolic rate equation for such kinetics.

$$\frac{d\eta}{dt} = \frac{k}{\eta} \quad (14)$$

where k is the reaction rate constant which depends on the diffusivities. This simple equation does not take into account various characteristics of the reactant powders such as particle size and shape, size distribution, contact area between particles, pack density and porosity in the green compacts. Hardt and Phung [34], assuming that the reactant particles are packed as alternating layers, showed that the reaction rate is given by

$$\frac{d\eta}{dt} = \frac{D}{w\alpha_o^2 \eta} \quad (15)$$

where D is the interdiffusion coefficient, $w = 1 + b_0/a_0$, a_0 and b_0 are half the effective particle sizes of A and B. Similarly, Jander [35] and Carter [36, 37] have derived expressions taking into account some of the powder characteristics and molar volume changes during the reaction.

In both solid–liquid [38] and solid–gas [39] reactions, if the molar volume of product AB is less than that of A, a porous product layer AB forms around A. Transport of reactant B (liquid or gas) to the surface of A for further continuation of reaction occurs through the porosity by convection or capillary action. The rate of such reactions is controlled by the surface-area of reactant A

$$\frac{d\eta}{dt} = kS \tag{16}$$

where k is the reaction rate constant. Such reactions are called topochemical.

On the other hand, if the molar volume of product AB is greater than that of solid reactant A, the product forms a protective layer around A and the reaction becomes limited by the diffusive transport of reactants through this product layer. Such reactions essentially follow the parabolic reaction rate given in Equation 14

In solid–gas reactions, when the molar volume of product AB is greater than that of A, a slightly different equation, taking into account the partial pressure of the gaseous reactant, is followed.

$$\frac{d\eta}{dt} = kSp_B \tag{17}$$

where S is the surface area of A and p_B is the partial pressure of B in the system and k is the reaction rate constant. This is a simplistic equation and several changes must be made depending on porosity level and tortuosity in the product, melting of solid reactant, etc. [39].

A special type of reaction is where a solid phase precipitates from a supersaturated solution of solid + liquid or liquid + liquid reactants. This is also referred to as solution precipitation reaction [40] and the rate is given by

$$\frac{d\eta}{dt} = k(1 - \eta)^n \tag{18}$$

where n is the order of the reaction.

2.3.2. Combustion wave structure

The generalized unsteady state Equation 7 can be simplified by steady state adiabatic approximation [17] into

$$\alpha\frac{d^2T}{dx^2} - v\frac{dT}{dx} + \frac{Q}{C_p}\phi(T, \eta) \tag{19}$$

$$-v\frac{d\eta}{dx} + \phi(T, \eta) = 0 \tag{20}$$

with the boundary conditions: $x = -\infty$, $T = T_o$, $\eta = 0$; $x = +\infty$, $T = T_{ad}$, $\eta = \eta_p$. In these equations, T_{ad} and η_p (often equal to 1) are determined by chemical thermodynamics, and solution of these equations gives us variation of temperature, heat generation and degree of conversion in the combustion region. Fig. 2 [17] shows a schematic picture of spatial distribution of these parameters along with the total enthalpy of the system. Conduction of the heat ahead of the wavefront ensures a steady rate of heat wave propagation.

As mentioned already, the profiles obtained (Fig. 2) are for a homogeneous system, with a stable wave propagation. But in many systems, a product layer separating the reagents can retard further interaction, leading to automatic breaking of the passage of the wave. In addition, diffusion processes in condensed systems can be so slow that the rate of conversion of reactants into products can be much slower compared to the rate of heat propagation. Assuming that the heat evolution in the SHS reaction can be expressed in terms of Equation 9, and solving Equations 19, 20 and 9 together [17], the wave structure shown in Fig. 3 is obtained. Here the reaction occurs over a wider zone. Maximum heat evolution occurs at temperatures much lower than T_{ad} and transformation much less

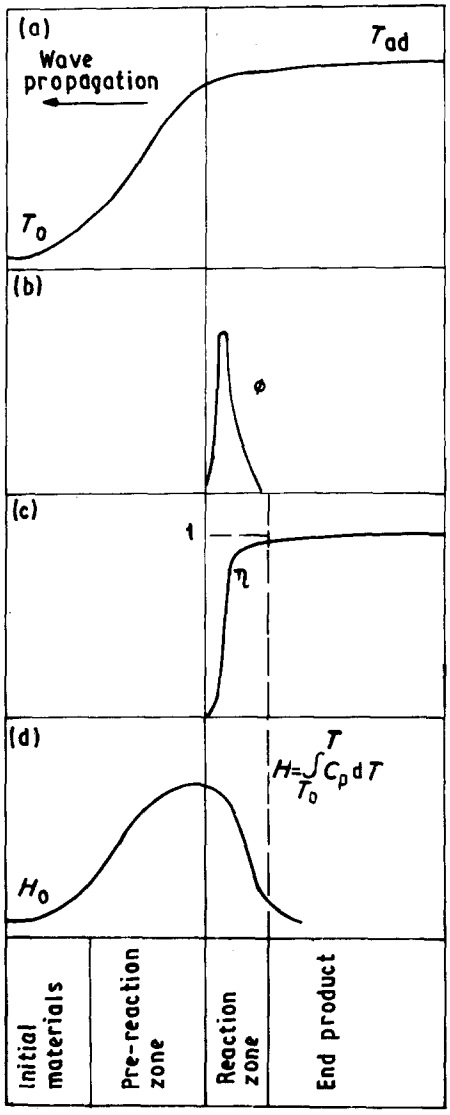

Figure 2 Spatial distribution of temperature, T, heat generated, ϕ, fraction converted, η, and enthalpy, H, in a homogeneous combustion wave [17].

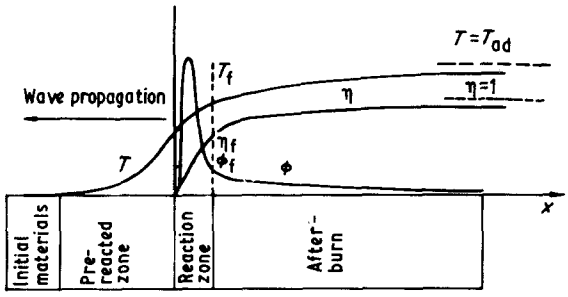

Figure 3 Combustion wave structure for heterogeneous combustion [17].

than unity. A long tail of afterburn is seen. This produces longer luminescence of the sample after passage of the wave. Two zones can be identified in this structure: high evolution of heat with high velocity of wave propagation followed by low heat evolution and higher level of transformation. This kind of structure explains how solid-phase gas-free combustion occurs in spite of extremely low values of diffusion coefficients in the solid phase (10^{-10}–10^{-5} cm^2 s^{-1}). Values of various parameters for different wave structures obtained in the formation of a number of metal borides are given by Zenin *et al.* [41].

A useful parameter numerically derived from these equations is [42]

$$\alpha_c = \frac{RT_{ad}}{E}\left(9.1\frac{C_p T_{ad}}{Q} - 2.5\right) \quad (21)$$

This delineates the combustion regimes. If $\alpha_c \geqslant 1$, steady state combustion occurs and if $\alpha_c < 1$, non-steady-state combustion occurs. In the steady state combustion, the wave velocity is constant and in the non-steady state combustion, oscillatory or spin combustion can occur. In the oscillatory mode, the wave propagates in successions of cyclic rapid and slow jumps, and in the spin mode, the wave propagation is in the form of a spiral encircling the sample at one or more reaction spots.

2.3.3. Velocity of wave propagation

From Equations 19 and 20, an expression for the velocity of wave propagation can be obtained

$$v^2 = \gamma(\eta_p)\alpha\left(\frac{C_p}{Q}\frac{RT_{ad}^2}{E}\right)k_o \exp\left(-\frac{E}{RT_{ad}}\right) \quad (22a)$$

where

$$\gamma(\eta_p) = \left\{\int_0^{\eta_p}[(\eta_p - \eta)/\phi(\eta)]\,d\eta\right\}^{-1} \quad (22b)$$

This expression shows the strong dependence of the velocity on the adiabatic temperature. A number of other parameters, not included in this expression, can also influence the velocity through changes caused in the adiabatic temperature. The above expression is derived assuming chemical reaction-controlled kinetics [24, 32]. A different expression, taking into account the dependence of particle size and the sample geometry is obtained by assuming diffusion kinetics [34]

$$v^2 = \frac{2\alpha}{d^2 s}D_o \exp(-E/RT) \quad (23)$$

where d is the particle size of one of the reactants and s is the stoichiometric ratio. These expressions are useful for obtaining the activation energies for different SHS reactions, elucidating the mechanisms operative during combustion.

3. Reaction mechanisms

3.1. Solid–solid reactions

As mentioned already, only a diffusion mechanism is possible in solid–solid reactions. Once the product layer forms between the reactants, further reaction proceeds by diffusion of reactant atoms across the product layer leading to slow reaction kinetics. For this reason, among the SHS reactions, the lowest combustion rates are found in solid–solid reactions. It is seen from Table II that the velocities of propagation for NbB_2, (solid–solid) combustion is 0.32–0.62 cm s^{-1}, whereas that for TiB_2 formation is 2–18 cm s^{-1} (solid–liquid). The effect of increasing the particle size on combustion for the Ta + C system was studied [43]. A high content of coarse fraction of metal in the reaction mixture acts like the addition of an inert diluent and leaves higher quantities of free carbon and unreacted metal in the product. This is further elaborated in the following section on solid–liquid reactions.

3.2. Solid–Liquid reactions

Solid–liquid reactions are common in SHS of several silicides, carbides and borides. In the case of carbides and borides, the metallic element is in the molten condition at T_{ad}, while in some silicide formation, silicon is in the molten condition. As pointed out by Sarkisyan [44, 45], for metal–silicon systems, $T_{ad} < 3000$ K while for metal–carbon and metal–boron systems, T_{ad} is in the range of 3000–4000 K. Hagg [46–48] classified these compounds based on the ratio of atomic radii, R_X/R_M, where R_X is the radius of the small non-metallic atom and R_M is the atomic radius of the transition metal. If this ratio is < 0.59, structures are simple and metal atoms occupy a lattice and the metalloid atoms are located interstitially. This happens for many carbides and borides while for silicides the ratio is > 0.59 resulting in complex crystal structures. Also, silicides have most complicated phase diagrams. In carbides, at best it is MeC, while in Me–Si and Me–B systems, a large number of different compounds including phases rich in non-metal can form. Lowering of the combustion temperature, brought about by a decrease in sample diameter or increase in metal particle size, leads to only incomplete reaction in carbides and borides, whereas, in the case of silicides it can also lead to inhomogeneity, with formation of several phases. This can result in a sharp fall in combustion velocity, which generally gives rise to oscillatory combustion.

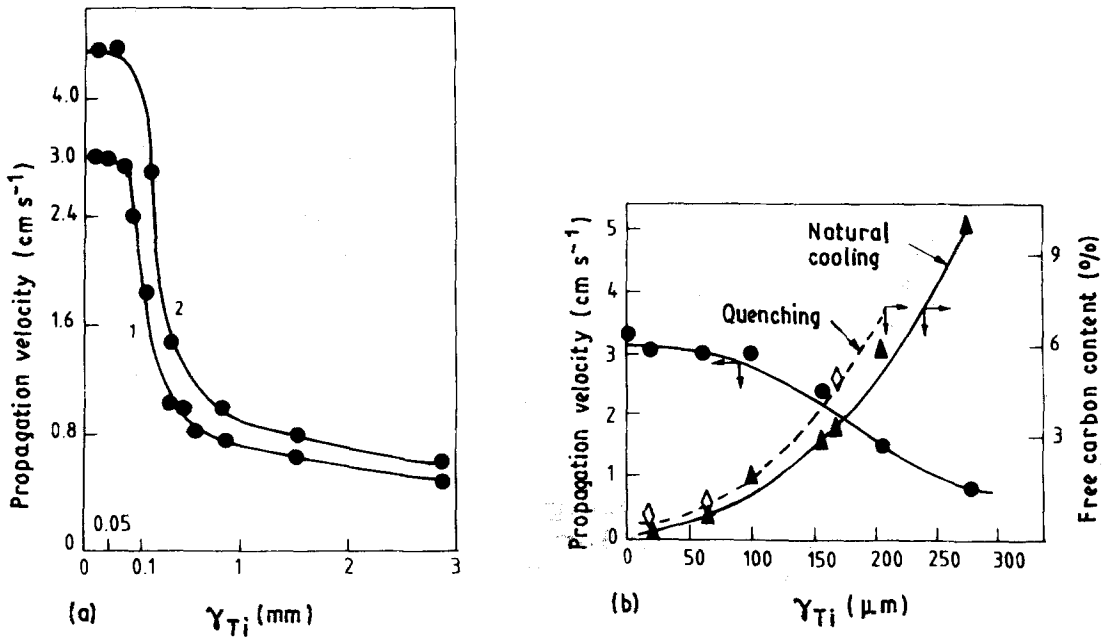

Figure 4 Variation of velocity of wave propagation and free carbon content with particle size of titanium in SHS of TiC: (a) coarse size range, (1) $T_0 = 20\,°C$, (2) $T_0 = 200\,°C$ [52], (b) fine size range [55].

The mechanism of SHS of TiC, which is typical of a solid–liquid reaction, has been studied extensively [49–56]. It was established that melting of titanium precedes the combustion reaction. In spite of this, it was experimentally observed [52, 55] that the velocity of combustion varies with titanium particle size (Fig. 4). Nekrasov [52] speculated that at large particle sizes ($r_{Ti} > 10^3$ μm), capillary spreading is the predominant mass transport mechanism, while with fine particle sizes ($r_{Ti} < 10^2$ μm) diffusion dominates. With this mechanism, it is difficult to understand how the particle size of the phase, which is in the molten condition at T_{ad} especially at fine particle size ranges, can control the reaction rates. In addition, capillary transport is expected to be much faster than the diffusion and hence must give higher combustion velocities. However, with Nekrasov's mechanism, capillary spreading is operative at large particle sizes, where experimentally lower combustion velocities have been observed (Fig. 4).

It was reported that the product morphology is independent of the initial particle morphology of titanium and carbon in the SHS of TiC [51]. Table VI [54] presents the dependence of combustion temperature and velocity on the particle size of titanium. Both decrease with increase in particle size. Fig. 4 shows the increase in free carbon content with increase in particle size. Free carbon content gives an indication of the incompleteness of the reaction.

These variations can only be explained by a solution–precipitation model proposed by Pampuch *et al.* for the Si–C system [40]. According to these authors, as the reaction front moves, repeated steps of dissolution of carbon in liquid silicon followed by precipitation of SiC from the liquid solution, occur successively. In the Ti–C system also, as discussed above, titanium melting precedes the combustion reaction as required by this mechanism. But this melting is confined only to a limited thickness on the particle surface as the particle size is increased, due to high thermal mass of larger particles. This reduces the combustion reaction, resulting in lower combustion temperatures. This leads to reduced conversion and lower combustion velocities, as the particle size is increased. This model also supports the experimental fact that the product morphology is independent of the initial particle morphologies.

TABLE VI Dependence of temperature and velocity of combustion of particle size of titanium [54]

Particle size of of titanium (μm)	Combustion temperature (exp.) (K)	Combustion rate ($cm\,s^{-1}$)
≪ 45	3070	3.6
125–160	2800	2.2
250–280	2660	1.3
Polydispersed	2753	1.1

The effect of increasing the particle size is similar to dilution as mentioned earlier. Fig. 5 [56] shows the microprobe analysis along the quenched TiC samples, with different initial particle sizes. When the titanium particle size is 45 μm, a narrow combustion zone with high degree of conversion is seen. As the particle size increases, the combustion zone widens and the conversion during after burn becomes significant.

The scheme presented in Fig. 6 summarizes the effect of different parameters on the combustion of a solid–liquid system and is useful is controlling SHS reactions. The parameters, enthalpy, initial temperature, dilution and particle size can be controlled so as to achieve a homogeneous combustion mode, with narrow reaction zone and the highest degree of conversion.

3.3. Liquid–liquid reactions

Many intermetallics and a few silicides form by this

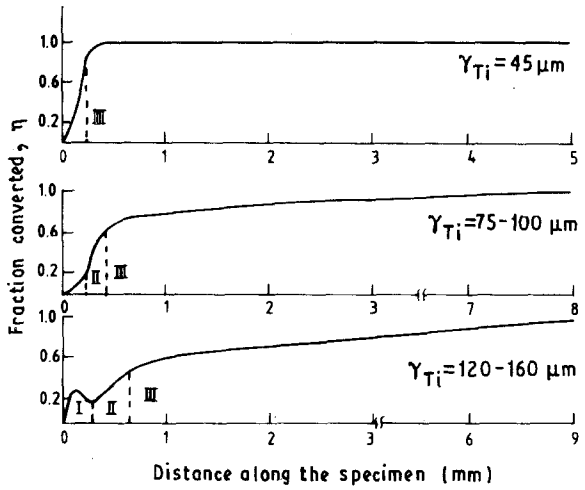

Figure 5 Variation of fraction converted into TiC along the length of samples quenched during SHS of TiC for different initial titanium particle sizes [56]. I, heating zone; II, propagation zone; III afterburn zone.

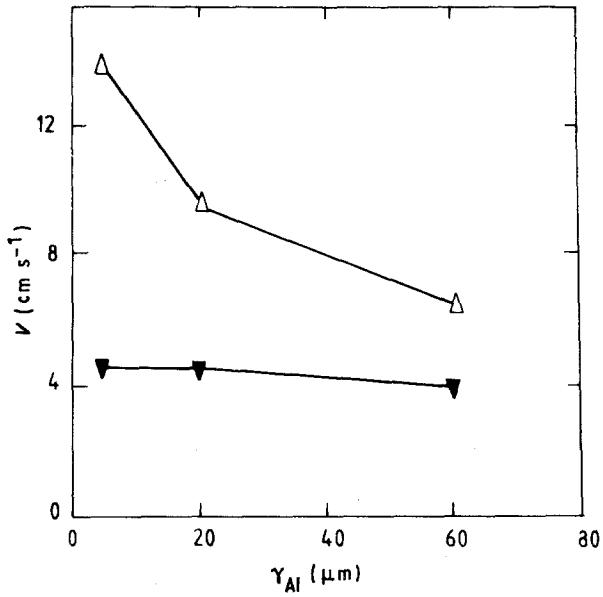

Figure 7 Effect of aluminium particle size on the combustion of NiAl [58]: (Δ) fine-grained and (▼) coarse-grained Ni.

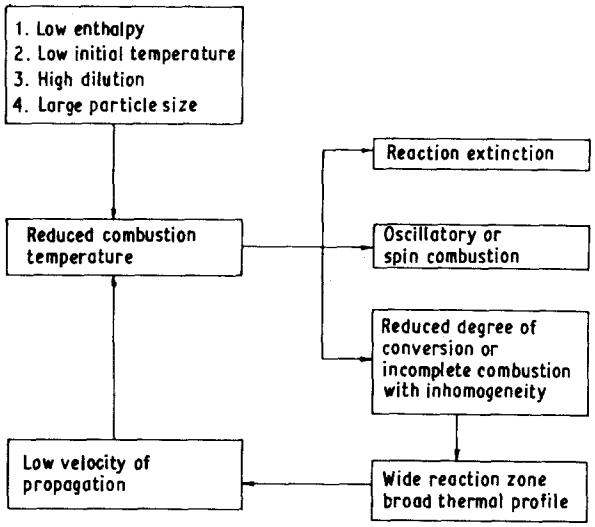

Figure 6 Effect of various parameters on the combustion of solid–liquid reactions.

reaction. The adiabatic temperature for many aluminides is low and usually it is necessary to heat the reactants to elevated temperatures to initiate the reactions. Owing to the availability of this additional heat, in most cases, the reactants are in the molten phase during combustion. The mechanisms of formation of NiAl has been studied in considerable detail [57–64]. Naiborodenko *et al.* [58] showed (Fig. 7) the dependence of combustion velocity on aluminum particle size for both coarse and fine nickel particles in the NiAl system. The combustion velocity is higher for fine nickel particles compared to coarse nickel particles. With fine nickel particles, the mechanism is essentially a liquid–liquid reaction with attendant high combustion velocity. Coarse particles lead to partial melting as mentioned earlier for solid–liquid reactions, affecting the reaction similar to dilution, thus resulting in lower combustion velocities. When the combustion temperature is equal to the congruent melting point of NiAl, the propagation velocity increases by three times [59]. Such higher velocities are probably due to higher reaction rates once the product is also in the liquid phase.

3.4. Solid–gas reactions

A large number of investigations were carried out on metal–nitrogen reactions [65–69] typical of gas-solid reactions. These reactions are highly exothermic, for example, T_{ad} for TiN formation is 4900 K. However, these high temperatures are not realized in practice due to lack of adiabaticity and also the tendency of the nitrides to dissociate well below these temperatures at atmospheric pressures. The metal–nitrogen systems have complicated phase diagrams with stable solid solutions, non-stoichiometric and stoichiometric nitrides. Due to these reasons, conversion of metal into nitride occurs only partially during the combustion wave passage. Further nitridation occurs during the after burn period.

Borovinskaya and Loryan [65] have shown (Fig. 8) the effect of nitrogen pressure on the conversion. As can be seen from Fig. 8, the nature of the product changes from solid-solution to TiN with increasing nitrogen pressure. Munir and Holt [66] have shown that pressures exceeding 2000 atm are required for complete conversion of many metals into nitrides, using the relation

$$\eta = (1/S) P_{N/2} \left[\frac{\pi}{(1-\pi)} \right] \frac{V_m}{RT} \qquad (24)$$

where P_{N_2} is the pressure of nitrogen gas, π initial porosity of the sample, V_m is the molar volume of the metal and S, the stoichiometric ratio of nitride (moles of nitrogen per mole of metal in the reaction).

Merzhanov *et al.* [67] derived a criterion to delineate the regimes, where the combustion is either chemical reaction rate controlled or gas permeation

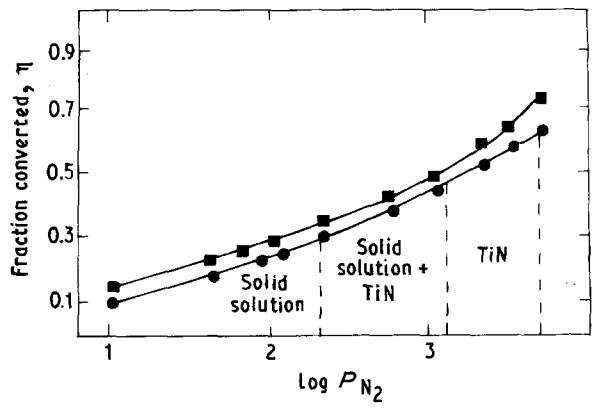

Figure 8 Effect of nitrogen pressure on the fraction converted for TiN combustion [65]. Green density: (■) 0.6, (●) 0.7.

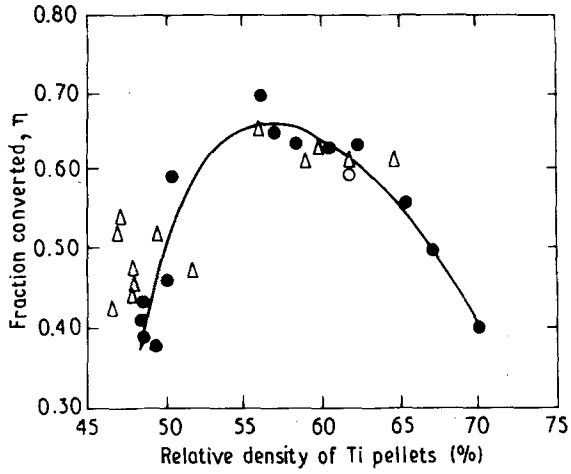

Figure 9 Dependance of fraction converted to TiN on the percentage of theoretical density of titanium compacts [68].

controlled. It is given by

$$P_c = \frac{4\nu RT_o}{\pi^2 M} \cdot \frac{Wd}{K_p P_{N_2}^2} \quad (25)$$

where P_c is the dimensionless criterion parameter, W the rate of nitrogen uptake by the metal ($g\,s^{-1}\,cm^{-2}$), d the diameter of the sample (cm), M the molecular weight of nitrogen gas ($g\,mol^{-1}$), K_p is the coefficient of permeability ($cm^2\,s^{-1}\,atm^{-1}$), P_{N_2} the pressure of nitrogen gas (atm), T_o the temperature of the the reactants and ν is the power in the relationship between the concentration of dissolved nitrogen and P_{N_2}. If $P_c \gg 1$, the reaction rate is determined by the gas permeation rate and the reaction occurs predominantly on the surface. If $P_c \ll 1$, the reaction rate is determined by chemical kinetics and the reaction occurs throughout the sample.

Apart from nitrogen pressure, the other important parameter affecting the solid–gas reactions is the reactant compact density. Eslaomloo-Grami and Munir [68] showed that the degree of conversion goes through a maximum as the relative density of titanium compacts is increased from 45% to 70% theoretical density (Fig. 9). At relatively low densities, melting of titanium metal reduces the gas permeability leading to a low degree of conversion. A similar situation results at high densities due to dense particle packing. Only at the intermediate density of 58%, is the highest degree of conversion noticed. The effect of both pressure and initial compact density on the degree of conversion is succinctly summarized in the form of a flow chart in Fig. 10. This figure is mainly based on the data obtained for metal–nitrogen systems. However, it should be relevant for other metal–gas reactions such as metal–hydrogen systems also. From Fig. 10, it can be seen that at low compact densities, conversion is high only if $T_{ad} < T_m$. At high compact densities, or if the $T_{ad} > T_m$ conversion is low. At high pressures, a reaction occurs throughout the sample giving a high conversion. At low pressures, if a dense reaction product forms on the surface, conversion is low.

4. Process techniques

4.1. Powder preparation

One of the simplest forms of SHS is the preparation of powders and this has been extensively reviewed earlier [12]. Here, only a brief description is given on the ignition characteristics, the purity of the products formed and the experimental parameters which affect such SHS reactions.

4.1.1. Ignition in SHS reactions

Rates of chemical reactions follow an Arrhenius type of behaviour as a function of temperature, increasing exponentially with the temperature. If a pellet of reactant mixture is heated slowly, the products form at a very low rate, and the heat of the exothermic reaction is dissipated because of losses to the surroundings. If, however, the rate of heating is sufficiently high so as to permit a reactant layer to rapidly attain a temperature where significant chemical reaction can occur, then the heat liberated by the reaction can further raise the temperature, thus facilitating faster and faster reaction. Such a positive feedback loop is schematically represented in Fig. 11 following Pampuch *et al.* [40].

Thus, as soon as the rate of the chemical reaction, and consequently, the rate of heat generation exceeds the rate of heat losses to the surroundings by conduction, convection and radiation, the reaction becomes self-sustaining. The temperature at which this transition occurs may be referred to as the "ignition temperature". Khaikin and Merzhanov [32] have rightly criticized the concept of ignition temperature, defined as a cut-off temperature below which the rate of the chemical reaction is zero, and above which rapid reaction starts, as devoid of any physical basis. In fact, such a definition can be valid only in systems where the activation energy is initially very high, and decreases abruptly as a consequence of the changes in the reaction mechanism following, for instance, a phase transformation like melting. The practical significance of the ignition temperature cannot, however, be overlooked, especially while selecting appropriate external heat sources for initiating SHS reactions.

All SHS processes are initiated by the rapid input of energy from an external source. A wide variety of initiation techniques are being used in practice. An

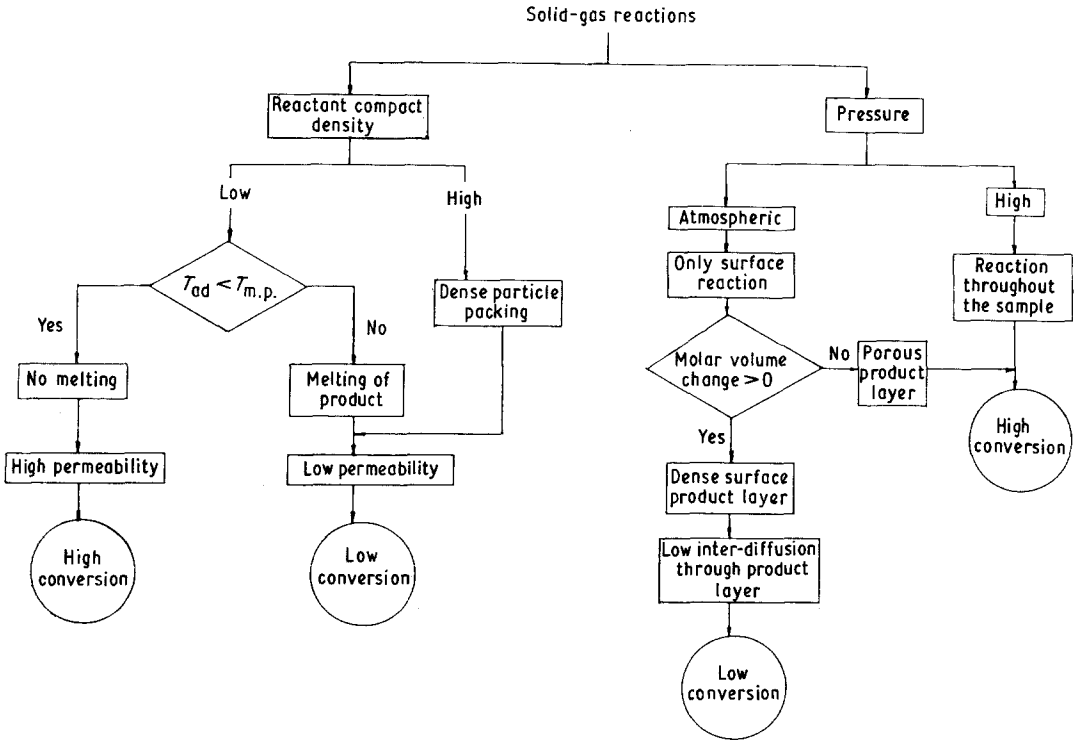

Figure 10 Effect of compact density and pressure on the degree of conversion in solid–gas reactions.

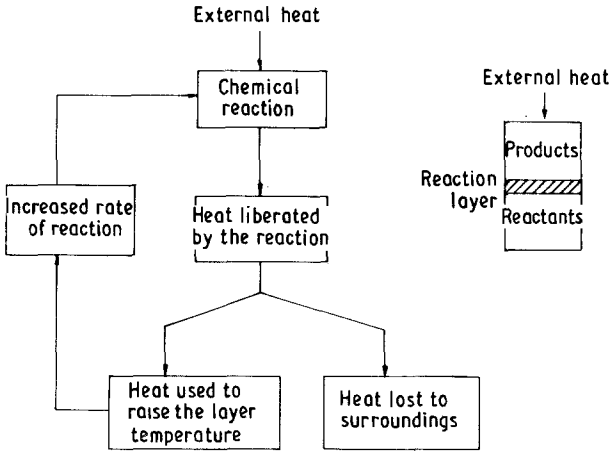

Figure 11 Positive feedback mechanism for self-propagation.

electric arc, electrically heated W/Mo filament, a magnesium ribbon, laser pulse, yet another highly exothermic reaction, rapid heating in a furnace, are but some of them. Depending on the experimental convenience, different types of ignition methods are used. For example, for initiation in an inert atmosphere or high/low pressure chambers, an electrically heated filament is the most commonly used technique. Such an external energy input must necessarily satisfy two requirements: (1) it must be able to raise the reactant layer to the ignition temperature, and (2) such an increase must be rapid enough to prevent any significant conversion of the reactants to the products before the ignition temperature is reached (pre-ignition reaction). A number of diverse factors such as the heats of reaction, thermophysical characteristics of the reactants and products, parameters controlling the reaction kinetics, etc., determine the type of the initiation process to be used. It has been reported that in many cases, ignition occurs once one of the reactants is in the molten state [72], although melting is not a necessary condition for ignition.

Few efforts have been made in the literature to quantify the concept of ignition [70, 71]. Assuming that the heat loss during ignition is due to conduction to the adjacent layers only, and that the reaction is diffusion controlled, Phung and Hardt [71] have modelled the ignition process. Analytical as well as numerical approaches for evaluating the ignition temperature are discussed. Based on these, they have estimated the initiation energy requirements for a number of reactions and compared with their experimental measurements. Such an exercise is useful in the theoretical prediction of ignition temperatures as well as in the parametric study of the ignition process itself. Korotkevich *et al.* [72] have studied the initiation process in a number of SHS systems using pulsed laser radiation and concluded that certain critical characteristics like the pulse energy and the average energy density define the conditions for ignition. In all the systems they have studied, ignition occurred with the appearance of a liquid phase. The authors also report that there exists a maximum value of the energy flux density beyond which the reactants simply vaporize and do not initiate the reaction.

4.1.2. Purity

Usually the SHS products show higher purity compared to the reactants involved in the reaction due to the evaporation of volatile impurities at the high combustion temperatures. Martirosyan *et al.* [73] studied the impurity levels in the reactants and products, by a d.c. arc emission spectral analysis, for

TABLE VII Spectral analysis of reactants and products of SHS [66].

(a) Silicides

Compound		Impurities (wt %)						T_{ad}(K)
		Mg	Ca	Mn	Sb	B	Cu	
$MoSi_2$	charge	0.004	0.012	0.0042	–	0.0056	0.0056	1920
	product	0.0038	0.012	0.0042	–	0.0056	0.0056	
$ZrSi_2$	charge	0.025	0.04	0.002	–	0.016	0.03	2100
	product	0.0007	0.02	0.001	–	0.004	0.018	
Ti_5Si_3	charge	0.05	0.15	0.0028	0.13	0.018	0.05	2500
	product	0.0009	0.028	0.0007	0.07	0.0002	0.0008	

(b) Carbides

Compound		Impurities (wt %)							T_{ad}(K)
		Mg	Ca	Cu	B	Mn	Pb	Sn	
Ta_2C	charge	0.014	0.031	0.0017	0.016	0.0086	0.0015	0.0028	2600
	product	0.011	0.022	0.001	0.011	0.006	0.0009	0.0018	
TaC	charge	0.01	0.03	0.0012	0.016	0.008	0.001	0.002	2700
	product	0.0084	0.022	0.0009	0.012	0.006	0.0008	0.0017	
TiC	charge	0.022	0.046	0.0012	0.065	0.0032	–	–	3210
	product	0.021	0.042	–	0.016	0.0028	–	–	
ZrC	charge	0.008	0.055	0.003	0.0028	0.0028	–	–	3400
	product	0.003	0.034	0.002	–	0.001	–	–	

(c) Borides

Compound		Impurities (wt %)							T_{ad}(K)
		Mg	Ca	Mn	Sb	Cu	Pb	Sn	
NbB_2	charge	0.02	0.008	0.004	–	0.013	–	–	2400
	product	0.0058	0.001	–	–	–	–	–	
TaB_2	charge	0.01	0.008	0.006	–	0.012	0.008	0.005	2700
	product	0.006	–	0.001	–	–	0.0001	–	
TiB_2	charge	0.0056	0.09	0.0028	0.007	0.012	–	–	3190
	product	0.001	0.04	0.0004	–	–	–	–	
ZrB_2	charge	0.003	0.06	0.0038	–	0.003	–	–	3310
	product	0.0002	0.028	0.001	–	–	–	–	
TiB	charge	0.003	0.056	0.0035	0.1	0.01	–	–	3350
	product	0.0006	0.025	0.0012	0.02	–	–	–	
HfB_2	charge	0.004	0.06	0.004	–	–	–	–	3520
	product	0.0001	0.015	0.0004	–	–	–	–	

systems with varying adiabatic temperatures. Table VII presents these data. No refinement occurs for $MoSi_2$ which has the lowest adiabatic temperature. The refinement process is enhanced with increasing T_{ad}, and is effective in removing only volatile impurities.

4.1.3. Experimental parameters affecting SHS

Several process variables affect the product quality and combustion velocity in SHS and these are discussed below [8].

1. Stoichiometric ratio: in general, any deviation from stoichiometric ratio reduces the T_{ad}. Non-stoichiometric mixtures are only used to make up the loss of any species due to volatilization during combustion.

2. Sample diameter: the combustion rate increases with the specimen diameter and remains constant after reaching a threshold value. This value depends on the combustion system. Lower combustion rates at low specimen diameters are a consequence of high radial heat losses.

3. Green density: thermal conductivity and specific heat of the green compact changes with the density of the compact. Consequently, the heat transfer in the combustion zone is different depending on the densities. At low densities, the heat in the combustion front is not effectively transferred to the pre-combustion zone, and this can lead to oscillatory combustion or extinction of the reaction. Similar results are obtained at high densities due to rapid heat transfer from the combustion zone. An optimum density of the compact is desired to obtain steady state combustion.

4. Particle size: the effect of particle size on combustion has been examined earlier while discussing reaction mechanisms. Fine particles are desirable for difficult-to-combust systems. In the formation of carbides and borides, increase in metal particle size tends to decrease the T_{ad} similar to dilution. The non-metallic powder used is usually very fine and is in the submicrometre range.

Table VIII presents the characteristics of some of the selected powders produced in the Soviet Union by SHS provided in pamphlets by Licensintorg, Moscow [74]. It is an impressive list of compounds with high

purities, little free non-metal content and fine particle size. Possible applications for each material suggested in these pamphlets are also included.

4.2. Combustion consolidation

4.2.1. Porosity generation in SHS reactions

As defined earlier, combustion consolidation refers to the process in which densification is carried out utilizing the exothermic heat available during or at the end of SHS reaction. Unlike in sintering, where the sample shrinks after the process, during the SHS, the product usually expands, increasing the porosity. Several attempts were made to clarify the origins of this porosity. Rice [75] distinguishes two types of porosity: (1) extrinsic and (2) intrinsic. Extrinsic porosity may be caused due to (a) the porosity in the green compact being carried over to the product due to lack of forces such as external pressure to cause shrinkage; (b) heterogeneous phase formation leading to Kirkendall porosity generated in microvolumes bringing about macroscopic expansion; (c) at high temperatures of combustion, outgassing of adsorbed gases and evaporation of volatile impurities occur. Combustion in the Ta + C system occurs in a "gas-less" way. However, Shkiro [43] reports a pressure dependence of the combustion rate in this system. This was attributed to the volatile impurities in the reactant mixture. Table IX presents the mass spectrometric analysis of the gases evolved during Ti–Si combustion [76]. The evolution of these gases during combustion is a major problem in consolidation of SHS products.

Porosity generated because of the molar volume change from reactants to products is termed intrinsic porosity. Table X presents the intrinsic volume and density changes in the formation of various SHS products from Rice [75]. For both elemental and thermite types of reaction, the volume change can be 15%–30%. Fig. 12 shows the expansion in the formation of $Al_2O_3 + TiB_2$ by thermite reaction. Thus the SHS products need external pressure application for densification.

Very little information is available in the open literature about the Soviet work on combustion consolidation. Frankhouser [8] presented a schematic representation (Fig. 13) of hot consolidation of Ti + C from a patent by Merzhanov *et al.* [77]. The Ti + C shapes are ignited by passing an electric current through the molybdenum electrodes between which the sample is placed. After combustion, the sample can be densified to 96% theoretical density by light mechanical compression. The following discussion about combustion consolidation is mainly based on the American and Japanese literature.

TABLE VIII Characteristics of powders obtained by SHS in Soviet Union [74]

Powder	Size (μm)	Metal content (%)	Non-metal content (%)	Free non-metal	Impurities	Specific surface ($m^2\ g^{-1}$)	Applications
Tic	1–200 polydispersive	77.0–79.5	18.0–19.8	0.2–2.0	O 0.5; Mg 0.06; Fe 0.1; Al 0.05	–	Abrasive
TiC	3–5	–	19.2–19.5	0.8 max	–	–	For hard alloys
B_4C	fine	B 74.0 min	20.0–20.3	–	B_2O_3 0.5 max; Mg 0.5 max	3.9	–
NbC	1–100	–	10.0–11.1	–	O 0.2 max	–	Hard alloys
TaC	1–160	–	6.0–6.1	0.2 max	O 0.2 max	–	Hard alloys
$TiC–Cr_3C_2$	1–125	Cr 24.0–25.0; Ti 55.9–56.0	17.0–17.1	0.5 max	–	–	Corosion resistant coatings, cutting tools and abrasives
β-SiC (N-doped)	–	–	27.0–27.8	0.8	N 2.0–4.0; O 1.0 max Fe 0.2 max	8–10	Heat resistant Structural ceramics and abrasive micro powders
TiB_2	1–200 Polydispersive	69.5–69.7	29.0–29.5	–	O 0.5 max	–	Used to produce corrosion resistant powder metallurgy products and to apply protective coatings
TiB_2	1–10	66.9–67.0	30.4–30.6	–	B_2O_3 0.2 max; Mg 0.3 max;	–	Super hard cutting tools
$MoSi_2$	1–50	61.9–62.5	35.5–36.5	0.3 max	O 0.3 max; Fe: 0.1 max;	–	Heating element upto 1700 °C
$TiSi_2$	1–100	44.0–44.5	51.9–52.0	–	O 0.1 max; Fe 0.1 max;	–	Protective coatings
TiN	1–200	77.0–78.5	20.3–21.5	–	O 0.5 max; Fe < 0.2	–	Hard alloys and cermets

TABLE VIII (*Continued*)

Powder	Size (μm)	Metal content (%)	Non-metal content (%)	Free non-metal	Impurities	Specific surface ($m^2 g^{-1}$)	Applications
HfN	1–50	92.0–94.0	5.9–6.0	–	O 0.5 max	–	Component in heat-resistant alloys, in high-ohmic resistors and as conductive material in thorium cathodes
TaN (cubic)	–	91.7–92.2	7.3–7.6	–	C 0.1 max; O 0.3 max	0.06	Microhardness = 3200 $kg mm^{-2}$ Electrical conductivity = 300 $\Omega^{-1} cm^{-1}$ component in hard alloys and electrical equipment
AlN	< 40	–	29.8–31.5	–	Al(free) 0.5 max; Fe 0.3 max	0.2–20.0	Heat-conductive dielectric material and high-temperature structural material
α-Si_3N_4	–	–	38.5–39.0	–	O 0.5 max; Si(free) 0.5 max; Fe 0.3 max; C 0.1 max;	1–3	Nozzles for spraying chemically active liquids, abrasives and tool materials
BN (Hex)	fine	–	53.0–53.6	–	B(free) 0.5 max; C 0.1 max; Mg 0.5 max	10	For synthesis of CBN, heat insulation and high-temperature lubricant
$TiC_{0.5}N_{0.5}$	2–125	–	N 10.8–11; C 10.1–9.2	C(free) 0.2 max	–	–	As a component in W-free hard alloys and as reinforcement in drilling tools
TiC-TiB_2	1–250	–	C 9.7–9.8; B 14.1–14.3	C(free) 0.15 max	–	–	–
Al_2O_3-TiC	classified fractions	Ti 33.5–37.9	9.4–8.0	C(free) 0.4 max	–	–	Used for making abrasive tools and polymer wear-resistant coatings to protect components of oil refining equipment.

TABLE IX Relative concentrations of various evolved species during SHS reactions in the Ti–Si system as a function of three titanium particle size [76]

Titanium powder size (mesh)	Gas volume (mol %)							
	H_2	CH_2	CH_3	OH	H_2O	$CO/N_2/Si$	O_2	CO_2/SiO
+ 200 − 100	95.42	trace	0.91	0.00	0.00	2.43	0.00	0.91
+ 325 − 200	89.84	trace	0.00	1.61	7.68	0.00	0.40	0.00
− 325	95.48	trace	0.38	trace	1.28	2.31	trace	0.00

4.2.2. Hot pressing and reaction hot pressing

Holt and Munir [20] attempted compaction of TiC in a 2.5 cm i.d. graphite die, heated rapidly to the ignition temperature of 1873 K under slight pressure. Thermal explosion occurs under these conditions raising the temperature of the sample to 3075 K. By rapid pressure application, samples could be densified to 95% theoretical density (TD). The main problem in hot pressing under thermal explosion conditions is the possibility of explosion if pressure is applied before the gas evolution is complete. Holt [11] reports preparation of 95%–98% TD TiB_2 and TiC by this method. He suggests that the heating rate should be fast enough to achieve spontaneous combustion throughout the volume of the compacts. This rate varies with chemical reactants and physical dimensions of the compact. Owing to the initial heat available in these processes, the combustion temperatures reached can be very high (cf. thermodynamics). This can result in a molten phase in the product and it can easily cause die failure. Dilution of the reactant with product phase minimizes this problem.

Richardson *et al.* [78] attempted hot pressing of TiC, TiB_2 and $TiB_2 + Al_2O_3$ in cold and hot graphite

TABLE X Intrinsic molar volume and density changes in the formation of ceramic and intermetallic products [75]

Product	V(%)	ρ_P/ρ_R^a
Single ceramic products from elemental reactions		
$MoSi_2$	− 40.6	1.39
SiC	− 28.4	1.39
$TiSi_2$	− 27.5	–
TiC	− 24.4	1.32
WC	− 23.8	1.31
TiB_2	− 23.3	1.29
TiSi	− 22.9	–
VC	− 21.0	1.27
$ZrSi_2$	− 20.9	1.26
ZrB_2	− 20.4	–
VB_2	− 19.2	1.24
NbB_2	− 19.1	1.24
NbC	− 17.4	–
ZrC	− 17.0	–
Cr_3C_2	− 16.9	–
TaC	− 15.1	1.18
CaB_6	− 14.8	1.17
W_2C	− 9.7	1.11
B_4C	− 8.3	1.09
AlB_{12}	− 6.3	1.07
BaB_{12}	− 4.2	–
Al_4C_3	− 1.7	1.02
Single intermetallic products from elemental reactions		
$MnBi_2$	− 78.1	–
NiAl	− 12.6	–
TiAl	− 5.3	–
Ni_3Al	− 5.2	–
Re_2Hf	− 2.2	–
Zr_2Be_{17}	− 1.8	–
Multiple products		
$3TiC + Al_2O_3$	− 22– − 28	1.28–1.39
$3TiB_2 + 5Al_2O_3$	− 27– − 28	1.37–1.39
$9Fe + 4Al_2O_3$	− 22	1.28
$3Fe + Al_2O_3$	− 19	1.23

[a] ρ_P, theoretical density of products; ρ_R, theoretical density of reactants.

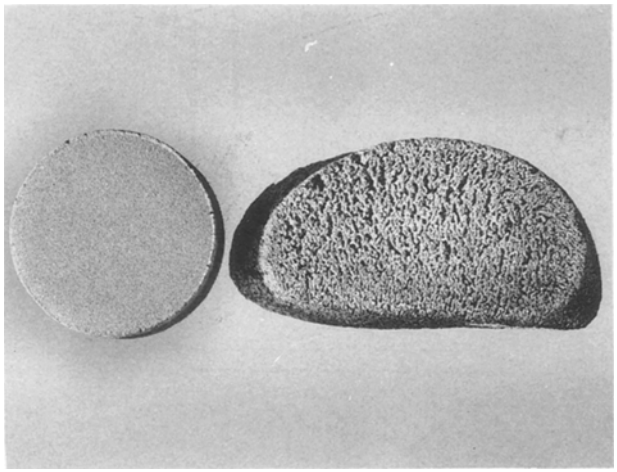

Figure 12 Expansion on ignition of ($TiO_2 + B_2O_3 + Al$) compact: (a) green compact (22 mm diameter); (b) ignited product ($Al_2O_3 + TiB_2$).

dies (3.8 cm i.d.). The samples were placed in the graphite dies under pressure and ignited. Once the reactants are ignited, the pressure falls by 50%, and is again increased to 100%. In certain cases, the temperature of the die is increased to 1273 K before ignition

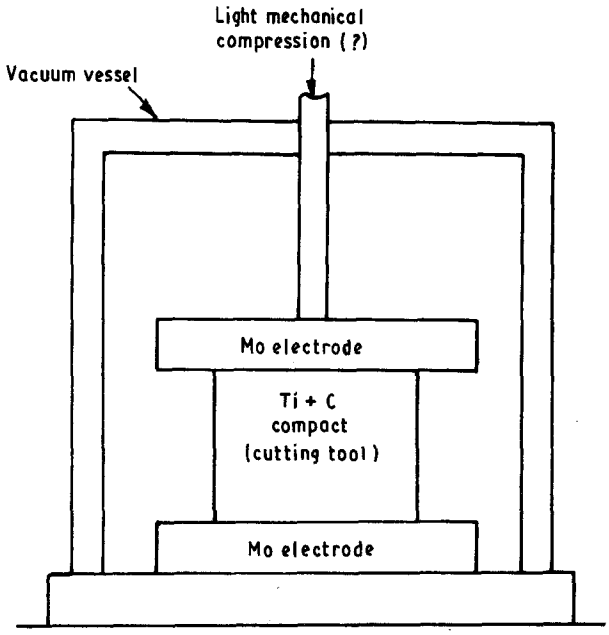

Figure 13 Schematic representation of hot consolidation of (Ti + C) [77].

using an induction furnace. In general, the resulting samples are non-uniformly densified with greater density at the centre compared to outer edges. The major problem is the evolution of gaseous species attributed to the oxide layers on the reactant particle surfaces. The problem is more severe in Ti + B systems compared to Ti + C, due to higher adiabatic temperatures in the former case, resulting in a more vigorous reaction.

Recently, Cameron *et al.* [79] prepared Al_2O_3-based composites both by conventional hot pressing (CHP) and reaction hot pressing (RHP). Here, the term reaction hot pressing is used when a spontaneous combustion reaction does not take place. In CHP, non-oxide powders are mixed with 0.3 μm α-Al_2O_3 and hot pressed. The hot pressing was carried out under vacuum or argon atmosphere at 1873–2073 K and 7–28 MPa for times up to 1 h. As shown in Table XI, the properties obtained by both processes are comparable. The low cost of raw materials is a major advantage in RHP [80].

4.2.3. Shock wave consolidation

Holt [11] tried simultaneous synthesis and consolidation of TiB_2 utilizing shock waves unsuccessfully. In another experiment he tried densification by striking a steel projectile at a velocity of 100 m s^{-1} immediately after the completion of the reaction. Here it was possible to consolidate the products just after the outgassing is completed. TiC and TiB_2 were densified to 95%–97% TD by this process, but the samples contained cracks. TiB_2 + Fe and TiC + Al_2O_3 were densified to 99% TD without any cracks, probably due to the presence of the liquid phase in the latter systems.

Recently, Kecskes *et al.* [81, 82] reported consolidation of TiC, TiB_2 and HfC by combining SHS reactions with dynamic compaction. They termed it

TABLE XI Comparison of properties of composites produced by conventional hot pressing (CHP) and reaction hot pressing (RHP) [79]

Phase composition (vol %)	Process	Density ($g\,cm^{-3}$)	Fracture strength (MPa)	Vickers hardness ($kg\,mm^{-2}$)	Sonic modulus (GPa)	Electrical resistivity (Ω cm)
1. 75 Al_2O_3 + 25 TiB_2	RHP	3.94 (95%)	330	2200	413	2.6×10^{-3}
	CHP	4.06 (98%)	360	2050	416	4.0×10^{-4}
2. 31 Al_2O_3 + 69 TiB_2	RHP	4.18 (96%)	350	2200	426	2.2×10^{-5}
	CHP	4.25 (97%)	320	2400	531	2.1×10^{-5}
3. 58 Al_2O_3 + 42 TiC	RHP	4.33 (99%)	600	2100	390	2.9×10^{-4}
	CHP	4.33 (99%)	510	2450	400	6.2×10^{-2}
4. 63 Al_2O_3 + 37 B_4C	RHP	3.47 (96%)	530	1990	342	0.97
	CHP	3.57 (99%)	360	2025	370	1.03

SHS/DC, in which a hot and porous body, produced by SHS, is densified while hot, by the action of a pressure wave generated by the detonation of a high explosive. This process is claimed to be cost effective for large samples.

Fig. 14 [82] shows the general arrangement used in SHS/DC. The reaction vessel consisted of a steel containment fixture and gypsum plasterboard package. Vent holes were provided for letting out the gases generated during the reaction. The compact was thermally insulated with zirconia felt. The assembly was placed on the top of 2 m tall sand pile. It was driven by the detonation into the pile, where the samples were allowed to cool slowly. This study had established that the SHS/DC process can produce dense product of TiC and TiB_2 of 98% TD and microhardness values which are equal to or greater than the commercially available hot-pressed materials. In general, a non-volatile impurity such as iron, originating from the reactants, remains in the product and segregates to the grain boundaries. This can weaken the inter-grain bonding, limiting the use of this material at high temperatures. In the case of TiC, densification improves with decreasing C/Ti ratio while microhardness falls. Optimum hardness and density are achieved for C/Ti ratios of 0.9–0.95. Even though TiC and TiB_2 could be densified to 98% TD, HfC could be densified only to 74%–87% TD. In addition, the product exhibited cracking and non-uniform intergranular bonding.

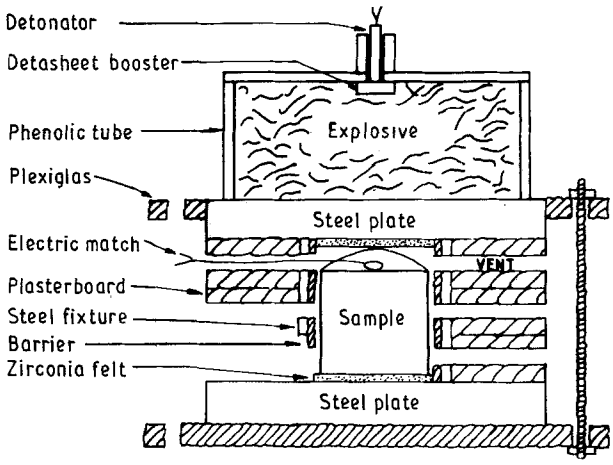

Figure 14 Schematic representation of SHS/DC [82].

4.2.4. Hot isostatic pressing and high pressure self combustion sintering (HPCS)

Holt [11] attempted isostatic compaction of Ti + 2B sealed in tantalum cans of 2.5 cm diameter and 2.5 cm height. These were ignited under an argon pressure of 101 MPa. Release of adsorbed gas developed a pressure of 300–600 MPa and blew holes in the container.

Japanese research workers developed a process of consolidation under very high pressures and termed it HPCS [83–87]. In their early experiments [83, 84], they subjected the samples, charged in a pyrophyllite cubic cell to a pressure of 3 GPa by means of a cubic anvil press. However, in later experiments, they used a gas pressure as illustrated in Fig. 15. Reactant powders are pressed into pellets and vacuum sealed into borosilicate glass containers in a similar way as used in HIPing. This container is placed in a combustion agent, in a graphite container and then placed in a high-pressure chamber. The combustion agent provides the heat required: e.g. Ti + C reaction can give a temperature of about 3200 K (chemical furnace).

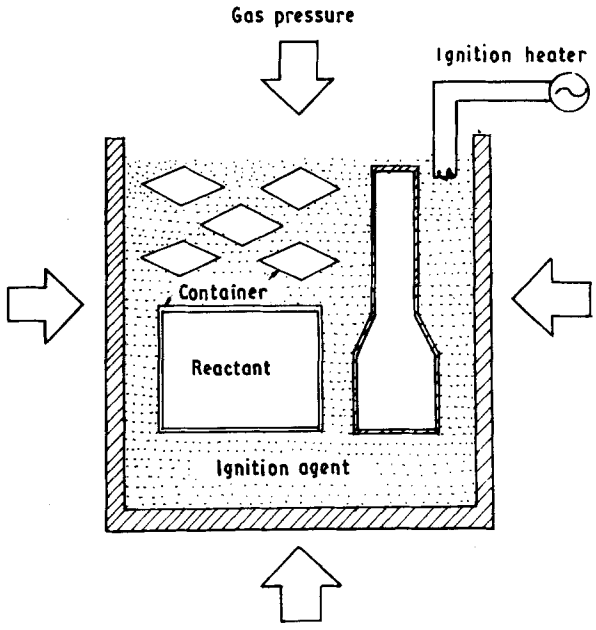

Figure 15 Schematic representation of HPCS [87].

The process is initiated by heating the pressure vessel to 973 K to make the glass container soft and 101 MPa argon pressure is applied. The combustion agent is subsequently ignited which in turn ignites the reactant pellets converting them into dense products within a few minutes. Techniques to overcome the gas evolution problems have not been mentioned by these authors. TiB_2, TiC, TiC–Al_2O_3, TiB_2-Ni and TiC–Ni have been compacted to near-theoretical-density using 101 MPa gas pressure. A list of material produced by this method is presented in Table XII [87]. At present, 30 mm diameter (or length) specimens are prepared, though the process was claimed to be amenable for mass production of near-net shape components. A new class of composites, known as "functionally gradient materials" (FGM) have been developed by this technique.

4.2.5. Hot rolling

Rice *et al.* [88, 89] conceived hot rolling of ceramics during the SHS reactions. In the process, the reactant powder mixture is loaded in a metal tube with a covering of graphite paper and a thin Al_2O_3-based felt material. The metal tubes containing reactant powders were cold rolled to 60%–70% TD. High densities could be obtained by cold rolling. However, such high density green compacts either cannot be ignited, or if ignited, will soon become extinguished due to their high thermal conductivity. The necessary roll speed was determined after measuring the reaction propagation rates. The tubes were outgassed in vacuum at 673–873 K prior to rolling. The tube was kept connected to a vacuum system throughout its processing for outgassing during reaction. This necessitated a special ignition procedure under vacuum. Two systems were considered. TiC + 20 vol % excess titanium and Al_2O_3 + TiB_2. In both cases, products obtained were of poor quality with high porosity and cracks.

4.2.6. General remarks on combustion consolidation

From the available research data, it is obvious that the process for consolidation of ceramics utilizing the exothermic heat is in its infancy. It is also probable that some aspects of development of consolidation techniques are not available in the open literature because of their commercial importance. One of the successful processes seem to be HPCS, where a pressure of 3 GPa is used for consolidation. Major limitations are the small size of the products that can be prepared with the process and the need for highly expensive high-pressure equipment. However, composites like FGMs can be prepared for specialized applications. The SHS/DC process, combining explosive forming with SHS, is claimed to be cost effective for large samples. Using this process, high density TiC and TiB_2 were obtained, but HfC could be densified only to a maximum of 87% TD showing the system dependence of the process. Major problems can be cracking and non-uniform density especially for large-sized samples. Processing of SHS products in cold or hot dies and reaction hot pressing have promise, if crack-free samples can be obtained. Cost saving is definitely possible in case of Al_2O_3-based composites such as Al_2O_3 + TiC and Al_2O_3 + TiB_2. Using RHP, these composites can be prepared with properties equivalent to that of CHP. Hot rolling combined with SHS reactions needs further research to obtain reasonably good samples.

Application of pressure during the reaction, generates the porosity in the product due to outgassing. Application of rapid rate deformation within 1 s after the completion of the reaction is possible only in processes like dynamic compaction. In SHS/DC of HfC, the explosives were detonated approximately 8 s after the SHS reaction was initiated because they found that the HfC reaction is completed in 5 s. The gap of 3 s can bring about considerable non-uniformity in temperature. On the other hand, it is possible to detonate just after 5 s as the reaction should be complete by this time. However, in SHS reactions, a small time lag is noticed between the initiation and beginning of the propagation of the reaction [90]. This can result in detonation before completion of reaction with consequent porosity. Thus the process control needs close attention in SHS/DC. This problem can become even more severe in mechanical and hydraulic pressing, due to the limitations on the maximum speeds achievable in these presses.

The process envisaged in combustion consolidation is the densification of a highly porous body, under temperatures, which are monotonically decreasing with time and spatially non-uniform. Frost and Ashby [91] outlined the deformation mechanism maps for dense ceramics like TiC and ZrC. From these maps one can obtain temperature–strain rate regimes under which these materials can be hot worked. The hardness of these carbides decreases rapidly between 0.2 and 0.4 T_m and at 0.5 T_m, these compounds are sufficiently soft for hot working. This shows that the combustion temperatures are adequately high for hot deformation. However, the SHS product just after reaction is highly porous and the temperature is non-uniform with steep gradients. Fig. 16 [92] shows the calculated temperature profiles of SHS product immediately after combustion, kept in a 10 cm diameter cold die. It can be seen that the temperature profile begins to become non-uniform just 2 s after completion of the reaction and becomes completely non-uniform after 36 s. The temperature falls rapidly to 1250–2700 K range from 2000–2700 K range within 1.5 s. Under these conditions the deformation mechanism can be entirely different from the data presented

TABLE XII Advanced ceramics and intermetallic compounds being produced by SHS in Japan [87]

Ceramics	Tic, TaC, HfC, SiC, B_4C, TiB_2, ZrB_2, Si_3N_4, AlN, SiAlON, BN, TiN, TaN, NbN, $MoSi_2$, TiSi, MoS_2, $MOSe_2$, CdS
Intermetallics	TiNi, TiAl, NiAl, CoAl
Composites	$3SiO_2 + 4Al + 3C \rightarrow 3SiC + 2Al_2O_3$ $SiO_2 + 2Mg + C \rightarrow SiC + 2MgO$ $2Ti + 2B + C \rightarrow TiC + TiB_2$

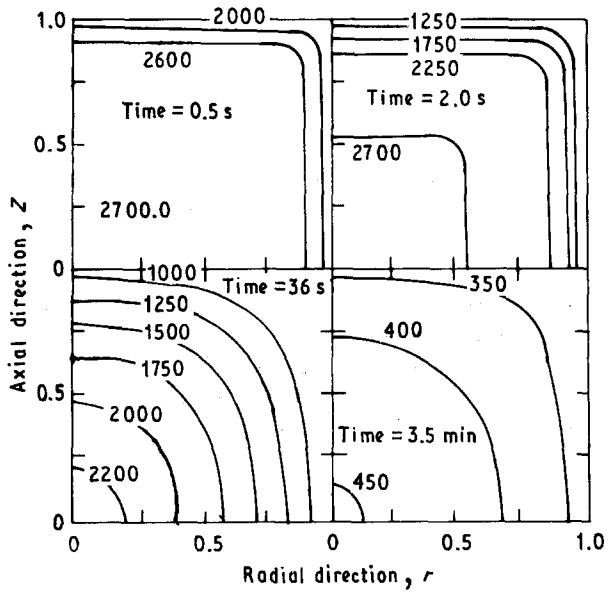

Figure 16 Calculated two-dimensional temperature distribution in an SHS compact at different times after combustion [92].

TABLE XIII Adiabatic temperatures and melting points of first product for certain highly exothermic reactions [12]

Reaction	T_{ad}, (K)	T_m(K)
1. $3Cr_2O_3 + 6Al + C = 2Cr_3C_2 + 3Al_2O_3$	6500	2163
2. $MoO_3 + 2Al + B = MoB + Al_2O_3$	4000	2820
3. $MoO_3 + 2Al + 2Si = MoSi_2 + Al_2O_3$	3300	2320
4. $3V_2O_5 + 10Al + 3N_2 = 6VN + 5Al_2O_3$	4800	2593

by Frost and Ashby [91]. More advanced techniques were developed [93, 94] to test metals for their workability. Some of these techniques with necessary modifications have to be adopted to combustion consolidation in order to obtain defect-free high-density products.

4.3. Combustion casting

One of the unique process adaptations utilizing SHS reactions is casting of refractory carbides, borides, nitrides and silicides. Examination of reactions in Table XIII reveals that the melting points of the products are lower than the adiabatic temperatures. Thus the products are in the liquid phase. Refractory compounds having a higher specific gravity, collect at the bottom on casting, while Al_2O_3 separates out as a slag layer on the top. In cases where the specific gravity difference is not sufficiently high, centrifugal force can be used to effect separation.

Most Soviet results on the casting of refractory compounds were patented [95]. Table XIV presents some data based on this patent. As very high temperatures are reached in these reactions, more volatile components can evaporate and the products can dissociate. This reduces the amount of non-metallic element in the combined form in the refractory compounds, thus lowering the product quality. Higher gas pressures during reaction prevent such dissociation and volatilization. Increased pressure also eliminates the violent escape of the reaction mixture from the reactor thus improving the yield. In addition, the product is free from pores and cavities as it solidifies under pressure. Nitrogen gas is used when a nitride is desired in the product, otherwise an inert gas such as argon is used for pressure application.

The centrifugal acceleration at 1 atm pressure can accelerate the separation process and also prevent violent escape of the reactant mixture, improving the yield. However, the combined non-metallic element value in the product does not improve significantly with centrifugal acceleration alone. High pressures are necessary to prevent dissociation and evaporation even at high centrifugal acceleration. In reactions, where the exothermic heat is not adequate to melt the products, supplementary heating can be provided.

TABLE XIV Characteristics of combustion-cast refractory inorganic materials [95]

Composition of starting mixture and expected product	Pressure (atm)	Centrifugal acceleration (g units)	Yield (%)	Combined carbon, (% theoretical)	Phases identified by XRD	Theoretical density (%)	Pores and cavities
1. 228 g MoO_3 + 12 g C	1	0	20	75	Mo_2C, Mo	99	yes
+ 108 g Al; Mo_2C	200	0	100	99.5	Mo_2C	96	no
	1	1000	100	78	Mo_2C.MO	98	no
	100	100	100	80	Mo_2C.Mo	97	no
	1000	1500	100	97	Mo_2C	97	no
2. 552 g V_2O_5 + 72 g C	1	0	30	43	VC, V_2C, V	98	yes
+ 270 g Al; VC	2000	0	100	94	VC, V_2C	96	no
	1	1000	100	50	VC, V_2C, V	98	no
	100	1500	100	88.5	VC, V_2C	96	no
3. 300 g CrO_3 + 24 g C	1	0	15	20	Cr_3C_2, Cr_4C, Cr	104	yes
162 g Al; Cr_3C_2	2000	0	100	97.6	Cr_3C_2	101	no
	1	1000	100	50	Cr_3C_2, Cr_4C Cr	102	no
	100	1500	100	82	Cr_3C_2, Cr_4C, Cr	101	no
4. 232 g WO_3 + 12 g C	5	0	100	60	WC, W_2C	93	no
+ 54 g Al; WC	2000	0	100	80	WC, W_2C	92	no
5. 288 g MoO_3 + 70 g	1	0	20	74	MoB, Mo_2B, Mo	102	yes
B_2O_3 + 162 g	2000	0	100	99.6	MoB	99	no
Al; MOB	1	1000	100	78	MoB, Mo_2B, Mo	102	no
	100	1000	100	96	MoB	99	no

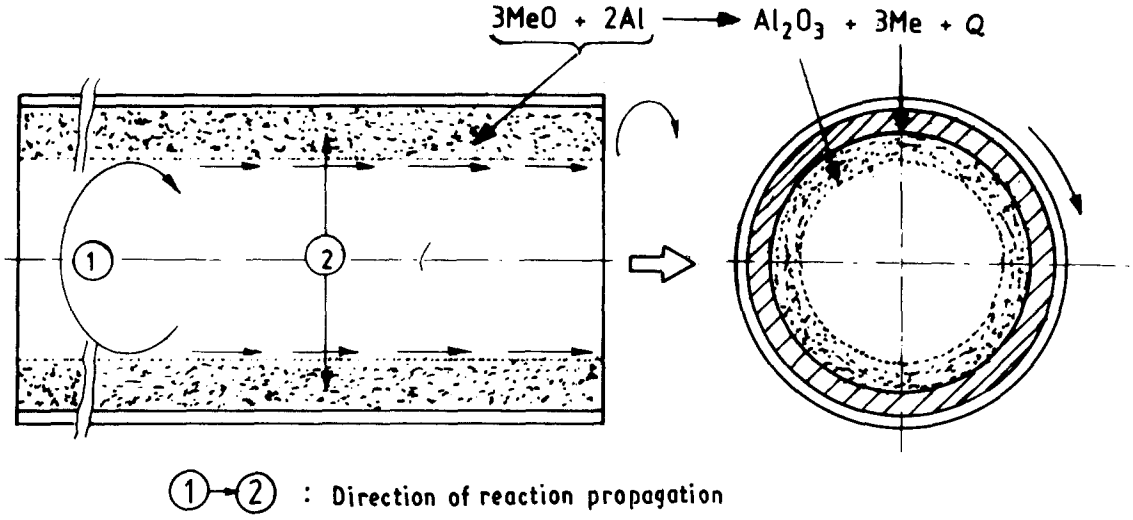

Figure 17 Schematic representation of the CT process [99].

Initial heating of the reactant mixtures to a temperture of 573–823 K was suggested for the preparation of tungsten carbide.

5. Novel techniques based on SHS

5.1. Centrifugal thermite (CT) process

Odawara [96–100] and his group in Japan developed a centrifugal thermite process for coating the inside of pipes. Fig. 17 gives a schematic representation of the process. Iron oxide and alumium mixture is placed inside the pipes and rotated at high speeds creating a centrifugal force (up to 130 g-units) on the mixture. Now the mixture can be ignited, utilizing an oxyacetylene flame. Reaction 4 propagates rapidly producing iron and Al_2O_3. This mixture is stratified due to the density difference between iron and alumina. A surface layer of alumina and an inner layer of iron is formed. The composite pipe has the strength and toughness of a metal and corrosion and abrasion resistance of a ceramic. The process provides a rapid (reaction completes in 15 s) and inexpensive method for producing such composite pipes. Pipes up to a length of 3 m have been coated by this process.

Various parameters were closely examined by Odawara [99]. An increase in the centrifugal force from 10 g-units to 200 g-units showed that the separation process improves with the increase in the centrifugal force. Above a centrifugal force of 200 g-units, the ceramic and metal forms uniformly with a clear boundary. A 5 mm thick ceramic layer of Al_2O_3 is formed on the surface and about 12 wt % hercynite ($FeO–Al_2O_3$) is formed at the boundary region. Properties of the ceramic layer produced by the CT process are compared with sintered Al_2O_3 in Table XV [99].

TABLE XV Comparison of properties of ceramic layer produced by CT process with sintered alumina [99]

Property	CT ceramic	Sintered alumina
1. Porosity (%)	5.6	–
2. Bulk density ($g\,cm^{-3}$)	3.86	3.80
3. Linear expansion coefficient (293–1273 K) (K^{-1})	8.57×10^{-6}	7.9×10^{-6}
4. Thermal conductivity (293 K) ($W\,m^{-1}\,K^{-1}$)	13.9	25.2
5. Resistivity at 293 K ($\Omega\,m$)	2×10^{7}	$> 10^{12}$
6. Hardness, H_v	1200	1650
7. Compressive strength (MPa)	> 850	2200
8. Bending strength (MPa)	140	310
9. Bulk modulus (MPa)	2×10^{5}	3.4×10^{5}

5.2. Combustion synthesis by mechanical alloying

McCormik and Schafer [101] in Australia devised a material synthesis process by a combination of mechanical alloying and SHS reaction. They selected highly exothermic reactions, like the reduction of copper oxide and zinc oxide with calcium metal. They milled these powder mixtures using WC balls in a steel vial. The vial temperature increased abruptly by 140 K after about 6 min milling. This shows the occurrence of a combustion reaction in the vial. However, the XRD pattern taken immediately after the reaction showed that the product contained some amount of CuO in addition to reduced copper. After 24 h milling, the product contained only Cu + CaO, indicating completion of reaction. The adiabatic temperature for calciothermic reduction of CuO is about 4000 K. A lubricant added to the milling mixture was considered to be effective to remove the heat, reducing the chances for spontaneous combustion. The spontaneous combustion is to be avoided in combustion milling in order to control the reaction and to obtain the desired products.

McCormic and his group are presently working to produce titanium and titanium alloy powders via the $TiCl_4$ + Mg route using this technique. He also feels that this is a viable technique to produce Fe–Nd–B magnets [102].

5.3. Functionally gradient materials

Functionally gradient materials [87, 103] are a new type of metal-reinforced ceramics with a gradual variation of metal content. Fig. 18 [103] illustrates a

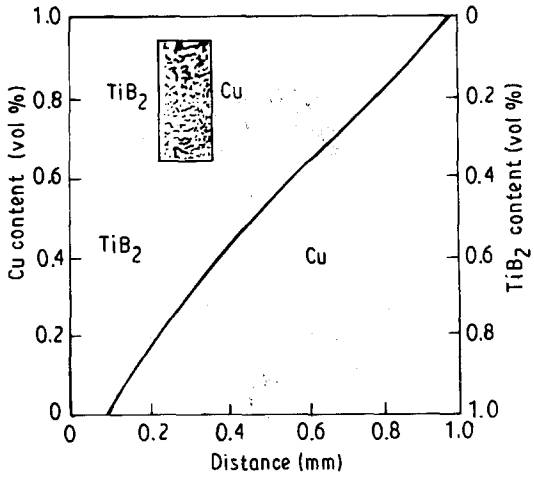

Figure 18 Calculated copper concentration profile in TiB_2–Cu FGM, assuming an infinite flat plate model [103].

TiB_2 + Cu composite, with 100% Cu at one end and 100% TiB_2 at the other, obtained by an infinitely flat plate model. These composites are supposed to have low internal thermal stresses and good fracture toughness.

SHS, in general, and HPCS, in particular, offers excellent opportunity to prepare such composites due to rapid combustion wave propagation with minimum diffusion. Two systems, TiC + Ni [87] and TiB_2 + Cu [103] have been studied in detail. For the preparation TiB_2 + Cu FGM, raw materials titanium copper and boron powders were mixed in a variety of proportions [103]. The powders were stacked with steps, compositionally divided into units of 2–21 and held at a pressure of 50 MPa for 30 min in vacuum. The compacts were ignited at a pressure of 25 MPa. The reaction involved is

$$Ti + 2B + aTiB_2 + bCu = (a + 1)TiB_2 + bCu \quad (26)$$

where a is the amount of additional TiB_2 added to the reaction for dilution and b is the copper content added to initial reactants. Fig. 19 [103] presents variation of T_{ad} with copper content, b, and TiB_2 content, a. With zero dilution, copper begins to boil at 60 wt % Cu and all the copper is boiled off at 25 wt % Cu. By dilution with TiB_2, T_{ad} can be kept below the boiling point of copper. A uniform T_{ad} throughout the different layers facilitates in obtaining a homogeneous microstructure. A smooth composition profile has been obtained by increasing the number of stacking units in the experimental study. In the centre of the samples, porosity was found to be higher. This may be related to evaporation of copper and the interaction of Cu + Ti in the reactants, forming intermetallics like CuTi. If some of these problems can be solved, unique materials can be produced.

5.4. Combustion-assisted synthesis of composites

5.4.1. Powder metallurgy route

Christodoulou *et al.* [104] patented a process termed XD, in which TiB_2 reinforcement particles form *in situ* in an aluminium matrix. Here elemental powders of titanium and boron are blended with aluminium powder and compacted. The compact is heated to about 1073 K, where the reaction between titanium and boron occurs exothermically leaving sub-micrometre TiB_2 particles in a matrix of aluminium. Table XVI shows the superior properties of the composites obtained by the XD process compared to that prepared by conventional methods [105].

5.4.2. Casting route

Ti–TiB–TiC composites were recently prepared by combustion-assisted synthesis by Ranganath *et al.* [106] via the casting route. Here conventional melting of titanium along with the following reaction

$$B_4C + (x + 5)Ti \rightarrow xTi + 4TiB + TiC \quad (27)$$

was used to prepare the composites. Fig. 20 shows the variation of T_{ad} with initial temperature for different excess moles of titanium (x in Equation 27). As is

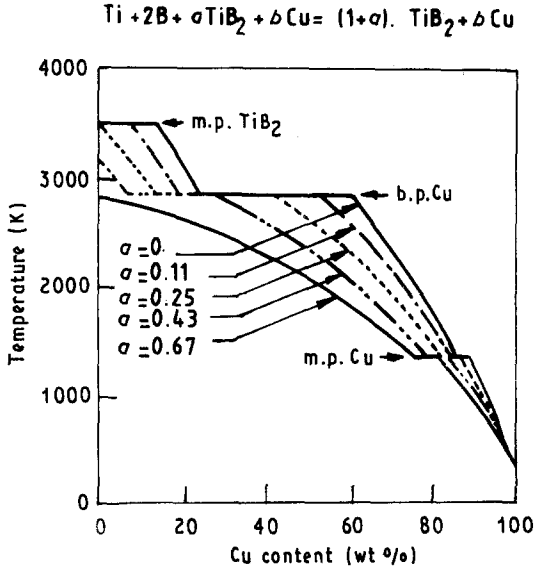

Figure 19 Variation of adiabatic temperature with copper content for different dilutions in the formation of TiB_2-Cu FGM [103].

TABLE XVI Comparison of tensile properties of Al–20 vol % TiB_2 composites processed by conventional methods and XD process [105]

Material	Modulus (GPa)	Yield strength (MPa)	Ultimate tensile strength (MPa)	Elongation (%)	Hardness H_v
1. Pure Al	70	64	90	21	37
2. Al–TiB_2 (conventional)	96	121	166	16	85
3. Al–TiB_2 (XD)	131	235	334	7	110

evident from Fig. 20, the ideal conditions for preparing these composites via the casting route are (1) to use initial temperatures below 1933 K to minimize decomposition of TiB, and (2) to keep T_{ad} above 1933 K so that all excess titanium added is in the molten condition. Well-dispersed fine particles of TiB + TiC in a matrix of titanium can be seen from the micrograph of these composites (Fig. 21).

5.4. Solution SHS

Patil *et al.* [107–109] have reported an innovative application of SHS process in the preparation of fine oxide powders from aqueous solution. The starting materials are the metal nitrate acting as oxidizer and a variety of organics such as urea, carbohydrazide, etc., serving as a fuel. The mixture of the two components is made into a pasty mass by dissolving in a minimum quantity of water. The reaction is initiated by introducing the paste into a furnace kept at 723 K. Various exothermic redox reactions, associated with the decomposition of nitrates and the oxidation of fuel, raise the temperature of the products to > 1873 K and the products foam and swell up in the container because of the large volume of gases produced. The whole reaction is complete within 5 min, typical of SHS reactions. The product mass is highly friable and yields homogeneous and fine-grained particles with an average particle size of approximately 3 μm. Clearly the distinctive advantages of the process are its simplicity, and the excellent means it provides for incorporating and uniformly distributing any desired dopants in the product oxide. In addition, the process is also safe and instantaneous. A number of oxide ceramics such as alumina with or without different dopants, ceria [107–109], superconducting materials such as $YBa_2Cu_3O_{7-\delta}$ [110] etc., have been synthesized by this technique.

The authors [107–109] report that many factors such as the rate of heating before ignition, stoichiometry, total mass of the reactant mixture and volume of the container used affect the process. In the preparation of alumina using aluminium nitrate, a heating rate of 100 K min^{-1} resulted in amorphous Al_2O_3 while higher heating rates gave α-Al_2O_3, thus indicating that preignition reactions in the former case have reduced the combustion temperature significantly. Similarly, urea-rich mixtures yielded alumina containing carbon impurity. A proper mass (of the mixture) to volume ratio is considered critical for initiating the process. Further systematic theoretical and experimental study of this interesting variant of the SHS reactions is desirable to improve the understanding of the process.

6. Summary and Critical appraisal and conclusion

Theoretical and processing aspects of the ongoing research in SHS are reviewed. Merzhanov's classification of SHS mechanisms, which provide a neat scheme for categorizing various SHS processes is presented. Simple thermochemical calculations give information on the order of temperatures attained, whether an SHS process is feasible, and what are the effects of parameters such as initial temperature and extent of dilution. However, in cases where the reactions are more complex, generalized equilibrium computation such as free energy minimization technique is required, in order to obtain the equilibrium composition as well as the adiabatic temperature.

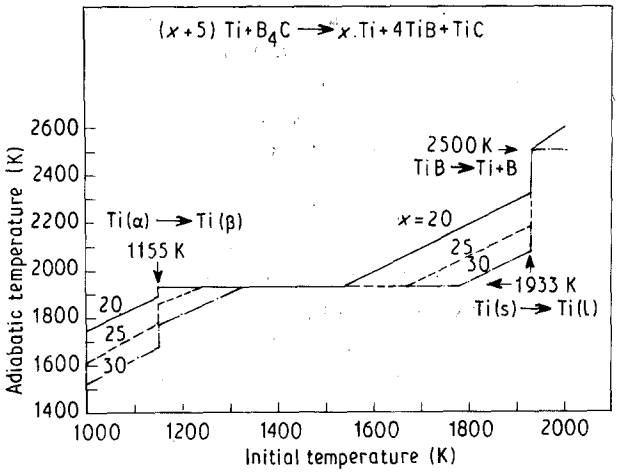

Figure 20 Variation of adiabatic temperature with initial temperature for different excess moles of titanium [106].

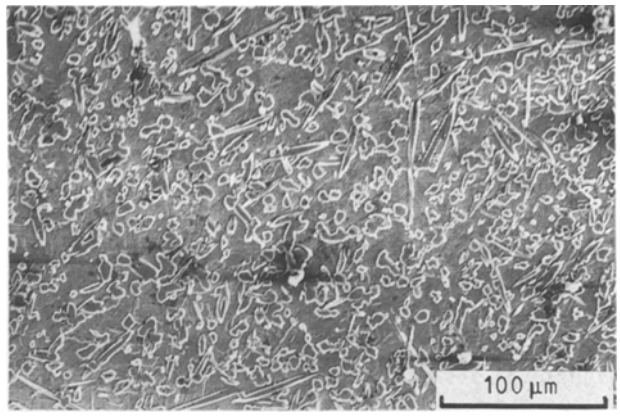

Figure 21 SEM micrograph of Ti-TiB-TiC composite produced by combustion-assisted casting [106].

More involved heat-transfer calculations taking into consideration the kinetics of reaction, can give an excellent idea about the modes of combustion, combustion wave structure, velocity of wave propagation, extent of conversion into products, etc. But then, a good deal of understanding about the reaction mechanism and kinetics is required as an essential input for such calculations. In addition. multiple equilibria must be taken into account wherever necessary. Such an integrated approach, involving heat and mass transfer and generalized equilibrium computation, in an iterative manner, has not been attempted so far.

In the processing by SHS, many a criticism exists regarding control of the process, purity of the products, degree of conversion, etc. [8]. However, Soviet scientists successfully produced a variety of ceramic powders by the process. Considerable effort is presently being made to obtain near net-shape products

using combustion consolidation, though vast improvements in the processing techniques are essential for any commercial exploitation. Several novel techniques based on SHS reactions, which hold great promise and show considerable commercial potential, are presently being developed.

Various advantages offered by the SHS process were mentioned earlier. Rice [80] gave a critical assessment of the technological and economic aspects of the process. According to him, one of the basic problems in the reaction processing is the choice of the mode of the reaction amongst the following: (1) self propagating reactions with local ignition; (2) spontaneous or volumetric reactions; (3) diffusional reactions. Here, both the considerations of kinetics and the conversion to products are to be examined. Further studies are desirable in order to obtain reaction yields in a particular system with all three modes of reaction. Economics for each of these modes are to be worked out taking into account large-scale production. Such an analysis can provide important data about the viability of an SHS process *vis-à-vis* the conventional reaction and diffusion processing for ceramic powder production.

In conclusion, the SHS process has come to a long way from the initial "pyrotechnic"-type experiments by Merzhanov and associates in material synthesis. Extensive research in the USSR has generated a basic understanding of the process and has resulted in the development of the processes for the production of a variety of ceramic powders. Further research and development, as well as a thorough cost-benefit analysis, is required before the process is widely accepted.

Acknowledgements

The authors thank Professor R. W. Cahn, University of Cambridge, UK, for his suggestion to write this review, Professor A. K. Lahiri, Indian Institute of Science, Bangalore, for many fruitful discussions on the theoretical aspects, and Dr P. Rama Rao, Director, D.M.R.L., for initiating SHS work in D.M.R.L. and for his keen interest throughout the preparation of this review.

References

1. A. G. MERZHANOV, V. M. SHKIRO and I. P. BOROVINSKAYA, "Synthesis of refractory inorganic compounds", of refractory compounds' (Noyes, New Jersey, USA, 1985).
2. *Idem.*, French Pat. 2088 668 (1972).
3. *Idem.*, US Pat. 3726 643 (1973).
4. *Idem.*, UK Pat. 1321 084 (1974).
5. *Idem.*, *Japan* Pat. 1098 839 (1982).
6. A. G. MERZHANOV and I. P. BOROVINSKAYA, *Dokl. Akad. Nauk. SSSR* **204** (1972) 336.
7. J. F. CRIDER, *Ceram. Engng Sci. Proc.* **3** (1982) 519.
8. W. F. FRANKHOUSER, K. W. BRENDLEY, M. C. KIESZEK and S. T. SULLIVAN, 'Gasless combustion synthesis of refractory compounds' (Noyes, New Jersey, USA, 1985).
9. L. M. SHEPPARD, *Adv. Mater. Proc.* **2**(2) (1986) 25.
10. J. W. McCAULEY, *Ceram. Engng Sci. Proc.* **11** (1990) 1137.
11. J. B. HOLT, *MRS Bull.* **12** (1987) 60.
12. Z. A. MUNIR, *Ceram. Bull.* **67** (1988) 342.
13. Z. A. MUNIR and V. ANSELMI-TAMBURINI, *Mater. Sci. Rep.* **3** (1989) 277.
14. A. G. MERZHANOV, in "Combustion and Plasma Synthesis of High temperature Materials", edited by Z. A. Munir and J. B. Holt (VCH, New York, 1990) p. 1.
15. H. C. YI and J. J. MOORE, *J. Mater. Sci.* **25** (1990) 1159.
16. A. G. MERZHANOV, in "Combustion Process in Chemical Technology and Metallury", edited by A. G. Merzhanov (Chernogolovka, 1975) p. 1.
17. A. G. MERZHANOV, *Fizik. Khim. Soverem. Problem.* (1983) 7.
18. I. P. BOROVINSKAYA, A. G. MERZHANOV, A. N. PITYULIN and V. S. SKEKHT, in "Combustion Process in Chemical Technology and Metallurgy", edited by A. G. Merzhanov (Chernogolovka, 1975) p. 113.
19. J. SUBRAHMANYAM, M. VIJAYAKUMAR, and S. RANGANATH, *Met. Mater. proc.* **1** (1989) 105.
20. J. B. HOLT and Z. A. MUNIR, *J. Mater. Sci.* **21** (1986) 251.
21. N. P. NOVIKOV, I. P. BOROVINSKAYA and A. G. MERZHANOV, in "Combustion Process in Chemical Technology and Metallurgy", edited by A. G. Merzhanov (Chernogolovka, 1975) p. 174.
22. F. VAN ZEGGEREN and S. H. STOREY, "The Computation of Chemical Equilibria" (Cambridge University Press, Cambridge, UK, 1970).
23. C. C. MAMYAN, YU. M. PETROV, L. K. STECEEK, in "Combustion Process in Chemical Technology and Metallurgy", edited by A. G. Merzhanov (Chernogolovka, 1975) p. 188.
24. B. I. KHAIKIN, *ibid.*, p. 227.
25. S. B. MORGOLIS, B. J. MATKOWSKY and M. R. BOTTY, in "Combustion and Plasma Synthesis of High temperature Materials", edited by Z. A. Munir and J. B. Holt (VCH, New York, 1990) p. 73.
26. A. BAYLIN and B. J. MATKOWSKY, *ibid.*, p. 61.
27. V. HLAVACEK, P. DIMITRIOU, J. DEGREVE and J. SCHOLTZ, *ibid.*, p. 83.
28. R. ARMSTRONG and M. KOSZYKOWSKI, *ibid.*, p. 88.
29. V. HLAVACEK, J. PUSZYNSKI, J. DEGREVE and S. KUMAR, *Chem. Engng Sci.* **41** (1986) 877.
30. J. PUSZYNSKI, J. DEGREVE and V. HLAVACEK, *Ind. Engng Chem. Res.* **26** (1987) 1424.
31. J. RAJAIAH, H. DANDEKAR, J. PUSZYNSKI, J. DEGREVE and V. HLAVACEK, *ibid.* **27** (1988) 513.
32. D. I. KHAIKIN and A. G. MERZHANOV, *ibid.* **2** (1966) 22.
33. C. WAGNER, *Z. Physik. Chem.* B34 (1936) 309.
34. A. P. HARDT and P. V. PHUNG, *Combust Flame* **21** (1973) 77.
35. W. JANDER, *Z. Anorg. Allg. Chem.* **163** (1927) 1.
36. R. E. CARTER, *J. Chem. Phys.* 34 (1961) 2010.
37. *Idem., ibid.* **35** (1961) 1137.
38. H. SCHMALZRIED, in "Treatise an Solid State Chemistry", Vol. 4, "Reactivity of Solids", edited by N. B. Hannay (Plenum Press, New York, 1976) p. 233.
39. A. W. D. HILLS, in "Heterogeneous Kinetics at Elevated Temperatures", edited by G. R. Belton and W. L. Worrel (Plenum Press, New York, 1970) p. 449.
40. R. PAMPUCH, J. LIS and L. STOBIERSKI, in "Science of Ceramics 14", edited by D. Taylor (The Institute of Ceramics, Shelton, Stoke-on-trent, Staffs., UK, 1988) p. 15.
41. A. A. ZENIN, A. G. MERZHANOV, G. A. NERSISYAN, *Combust. Explos. Shock Waves USSR* **17**(1) (1981) 63.
42. F. G. SHKADINSKI, B. I. KHAIKIN and A. G. MERZHANOV, *ibid.* **7** (1971) 15.
43. V. M. SHKIRO, G. A. NERSISYAN and I. P. BOROVINSKAYÁ, *ibid.* **14** (1978) 455.
44. A. R. SERKISYAN, S. K. DOLUKHANYAN, I. P. BOROVINSKAYA and A. G. MERZHANOV, *ibid.* **14** (1978) 310.
45. A. R. SERKISYAN, S. K. DOLUKHANYAN and I. P. BOROVINSKAYA, *Sov. Powd. Met. Met. Cer.* **17** (1978) 424.
46. G. HAGG, *Z. Phys. Chem.* **B12** (1931) 33.
47. *Idem., ibid.* **B11** (1930) 433.
48. A. WESTGREN, *J. Franklin Inst.* **212** (1931) 577.
49. S. G. VADCHENKO, Y. M. GRIGOREV and A. G. MERZHANOV, *Combust. Explos. Shock Waves USSR* **12** (1976) 606.
50. V. A. KNYAZIK, A. G. MERZHANOV, V. V. SOLOMONOV and K. S. SHTEINBERG, *ibid.* **21** (1985) 333.

51. A. S. ROGACHEV, A. S. MUKASYAN and A. G. MERZHANOV, *Dokl. Phys. Chem.* **297** (1987) 1240.
52. E. A. NEKRASOV, Y. M. MAKSIMOV, M. K. ZIATDILOV and A. S. SHTEINBERG, *ibid.* **14** (1978) 575.
53. A. I. KIRBYASHKIN, I. M. MOKSIMOV and A. G. MERZHANOV, *ibid.* **17** (1982) 191.
54. T. S. AZATYAN, V. M. MALTSEV, A. G. MERZHANOV and V. A. SELEZNEV, *ibid.* **13** (1977) 156.
55. V. M. SHKIRO and I. P. BOROVINSKAYA, in "Combustion Process in Chemical Technology and Metallurgy", edited by A. G. Merzhanov, (Chernogolovka, 1975) p. 253.
56. V. M. SHKIRO, V. N. DOROSHIN and I. P. BOROVINSKAYA, *Combust. Explos. shock Waves USSR* **16** (1981) 370.
57. Y. S. NAIBERDENKO, V. I. ITIN, A. G. MERZHANOV, I. P. BOROVINSKAYA, V. P. USHAKOV and V. M. MASLOV, *Sov. Phys. J.* **6** (1975) 872.
58. Y. S. NAIBERDENKO and V. I. ITIN, *Combust. Explos. Shock Waves USSR* **11** (1975) 293.
59. V. M. MASLOV, I. P. BOROVINSKAYA and A. G. MERZHANOV, *ibid.* **12** (1976) 31.
60. Y. S. NAIBERDENKO and V. I. ITIN, *ibid.* **11** (1975) 626.
61. B. V. BOLDYREV, V. V. ALEKSANDROV, M. A. KORCHAGIN, B. P. TOLOCHKO, S. N. GUSKO, A. S. SOLOKOV, M. A. SHEROMOV and N. Z. LYAKHOV, *Dokl. Akad. Nauk SSSR* **259** (1981) 1127.
62. V. V. ALEKSANDROV, M. A. KORCHAGIN, B. P. TOLOCHKO and M. A. SHEROMOV, *Combust. Explos. Shock Waves USSR* **19** (1984) 430.
63. K. A. PHILPOT, Z. A. MUNIR and J. B. HOLT, *J. Mater. Sci.* **22** (1987) 159.
64. Y. S. NAIBORDENKO, V. I. ITIN, B. P. BELOZEROV and V. P. USHAKOV, *Sov. Phys. J.* **16** (1973) 1507.
65. I. P. BOROVINSKAYA and V. E. LORYAN, *Sov. Powd. Met. Met. Ceram.* **17** (1978) 851.
66. Z. A. MUNIR and J. B. HOLT, *J. Mater. Sci.* **22** (1987) 710.
67. A. G. MERZHANOV, I. P. BOROVINSKAYA and Y. E. VOLODIN, *Dokl. Phys. Chem.* **206** (1973) 833.
68. M. ESLAOMLOO-GRAMI and Z. A. MUNIR, *J. Amer. Ceram. Soc.* **73** (1990) 1235.
69. A. N. PITYULIN, V. A. SHEHERBAKOV, I. P. BOROVINSKAYA and A. G. MERZHANOV, *Combust. Explos. Shock Waves USSR* **15** (1979) 432.
70. A. G. STRUNINA, T. M. MARTEM'YANOVE, V. V. BARZYKIN and V. I. ERMAKOV, *ibid.* **10** (1974) 449.
71. P. V. PHUNG and A. P. HARDT, *Combust. Flame* **22** (1974) 323.
72. I. I. KOROTKEVICH, G. V. KHIL'CHENKO, G. P. POLUNINA and L. M. VIDAVSKII, *Combust. Explos. Shock Waves USSR* **17** (1981) 61.
73. N. A. MARTIROSYAN, S. K. DOLUKHANYAN, I. P. BOROVINSKAYA and A. G. MERZHANOV, *Sov. Powd. Met. Met. Ceram.* **16** (1977) 522.
74. Pamphlets from LICENSINTORG, Moscow, Russia
75. R. W. RICE and W. J. McDONOUGH, *J. Amer. Ceram. Soc.* **68** (1985) c-122.
76. K. A. GABRIEL and J. R. ALEXANDER, in "Material Processing by Self-propagating High-temperature Synthesis (SHS)", edited by K. Gabriel, S. Wah and J. W. McCauley, MTL SP87-3, DARPA/Army Symposium Proceedings October 1985, p. 441.
77. A. G. MERZHANOV *et al.*, USSR Pat. 584052 (1975).
78. G. Y. RICHARDSON, R. W. RICE and W. J. McDONOUGH, *Ceram. Engng Sci. Proc.* **7** (1986) 761.
79. C. P. CAMERON, J. H. ENLOE, L. E. DOLHERT and R. W. RICE, *ibid.* **11** (1990) 1190.
80. R. W. RICE, *ibid.* **11** (1990) 1126.
81. L. J. KECSKES, T. KOHKE and A. NIILER, *J. Amer. Ceram. Soc.* **73** (1990) 1274.
82. L. J. KECSKES, R. F. BENCK and P. H. NETHERWOOD Jr, *ibid.* **73** (1990) 383.
83. Y. MIYAMOTO, M. KOIZUMI and O. YAMADA, *J. Amer. Ceram. Soc.* **67** (1984) c-224
84. O. YAMADA, Y. MIYAMOTO and M. KOIZUMI, *Amer. Ceram. Soc. Bull.* **64** (1985) 319.
85. S. ADACHI, T. WADA, T. MIHARA, Y. MIYAMOTO, M. KOIZUMI and O. YAMADA, *J. Amer. Ceram. Soc.* **72** (1989) 805.
86. S. ADACHI, T. WADA, T. MIHARA, Y. MIYAMOTO and M. KOIZUMI, *J. Amer. Ceram. Soc.* **73** (1990) 1451.
87. Y. MIYAMOTO, *Amer. Ceram. Soc. Bull.* **69** (1990) 686.
88. R. W. RICE, W. J. McDONOUGH, G. Y. RICHARDSON, J. M. KUNUTZ and T. SCHROETER, *Ceram. Engng Sci. Proc.* **7** (1986) 751.
89. R. W. RICE, *ibid.* **11** (1990) 1203.
90. J. SUBRAHMANYAM, unpublished.
91. H. J. FROST and M. F. ASHBY, "Deformation Mechanism Maps" (Pergamon Press, 1982) p. 90.
92. J. A. PUSZYNSKI, S. MAJOROWSKI and V. HLAVACEK, *Ceram. Engng Sci. Proc.* **11** (1990) 1182.
93. G. E. DIETER, in "Metals Handbook, 9th Edn, Vol. 14 (ASM International, Ohio, USA, 1988) pp. 363, 373.
94. S. I. OH, *Int. J. Mech. Sci.* **17** (1982) 293.
95. A. G. MERZHANOV, V. I. JUKHVID, I. P. BOROVINSKAYA and F. I. DOBOVITSKY, UK Pat. 1497025 (1978).
96. O. ODAWARA, US Pat. 4363832 (1982).
97. O. ODAWARA and J. IKEUCHI, *J. Jpn Inst. Metals Sendai* **45** (1981) 316.
98. *Idem., J. Amer. Ceram.* Soc. **69** (1986) c-85.
99. O. ODAWARA, *ibid.* **73** (1990) 629.
100. O. ODAWARA, in "MRS International Meet on Advanced Materials", Vol. 4 (Eds. M. Doyama, S. Somiya, R. P. H. Chang, Publ. Materials Research Society, Pittsburgh, Penn., USA, 1989) p. 535.
101. G. B. SCHAFER and P. G. McCORMIK, *Scripta Metall.* **23** (1989) 835.
102. P. G. McCORMIK, private communication 1990.
103. N. SATA, K. NAGATA, N. SANADA, T. HIRANO and M. NIINO, in "MRS International Meet on Advanced Materials", Vol. 4 (Eds. M. Doyama, S. Somiya, R. P. H. Chang, Publ. Materials Research Society, Pittsburgh, Penn., USA, 1989) 541.
104. L. CHRISTODOULOU, D. C. NAGLE and BRUPBACHER, Int. Pat. wo86/06366 (1986).
105. A. K. KURUVILLA, K. S. PRASAD, V. V. BHANUPRASAD and Y. R. MAHAJAN, *Scripta Metall.* **24** (1990) 873.
106. S. RANGANATH, M. VIJAYAKUMAR and J. SUBRAHMANYAM, *Mat. Sci. & Engg.*, A149 (1992) 253
107. J. J. KINGSLEY, N. MANICKAM and K. C. PATIL, *Bull. Mater. Sci.* **13** (1990) 179.
108. M. M. A. SEKHAR, S. S. MANOHARAN and K. C. PATIL, *J. Mater. Sci. Lett.* **9** (1990) 1205.
109. R. GOPICHANDRAN and K. C. PATIL, *Mater. Lett.* **10** (1990) 291.
110. R. GOPALAN, Y. S. N. MURTHY, T. RAJASEKHARAN, S. RAVI and V. SESHUBAI, *ibid.* **8** (1989) 441.

Received 14 May
and accepted 12 September 1991